

CHARACTERISATION OF A *DROSOPHILA* MODEL OF CARDIOVASCULAR  
DISEASE

CHARACTERISATION OF A *DROSOPHILA* MODEL OF CARDIOVASCULAR  
DISEASE

RACHEL M. ANDREWS

A thesis

Submitted to the School of Graduate Studies in Partial Fulfillment of the Requirements

For the Degree Master of Science

McMaster University © Rachel Andrews, August 2019

McMaster University, Master of Science (2019) Hamilton, Ontario (Biology)

Title: Characterisation of a *Drosophila* model of cardiovascular disease

Author: Rachel M. Andrews, BSc (Honours)

Supervisor: J. Roger Jacobs

Number of Pages: i - 82

## Abstract

The heart, as a vital organ, must pump continuously to deliver oxygenated blood to the tissues of the body. The physical stress of pumping is supported by the extracellular matrix (ECM), a dynamic protein scaffold inside and around the heart. While a regulated ECM is required to maintain heart function, aberrant or excessive ECM remodelling, called fibrosis, is associated with disease states and is a hallmark of cardiovascular disease. One major trigger of cardiovascular disease is obesity, and fibrotic remodelling is known to occur in this context. In order to study the impact of increased body size on heart function and the molecular and biophysical characteristics of the ECM, a larval overgrowth model for obesity in the genetic model *Drosophila melanogaster* has been developed and characterised. This model produces giant larvae twice as heavy as their wildtype counterparts, and allows a unique opportunity to study changes in the cardiac ECM in a simple genetic model. Results demonstrate a remarkable ability of the ECM to accommodate this increase in size. The muscles of the heart are particularly robust, and there are no obvious observable defects to the matrix. Preliminary results suggest Collagen fibres are thicker and more disperse. When observing heart functionality, the cross-sectional area of the heart lumen is increased significantly in giant larvae, both at diastole and systole. However, giant larvae display defects in contraction of the heart tube, characterised by an inability to contract fully at systole. This results in a less than proportional increase in stroke volume, and an increase in heart rate. Heart function of giant larvae is clearly affected by the increase in body size. To quantify the impact to the biophysical structure of the ECM, an atomic force microscopy protocol is being developed.

## Acknowledgements

I would like to begin by thanking my supervisor, Roger Jacobs. The completion of this degree would not have been possible without his never-ending support. Thank you for being patient as I visit your office for the fifty seventh time that day. Without your unwavering composure over the last few weeks this would not have come together.

Thank you to my committee member Ian Dworkin. Your input over the last two years has been very much appreciated. Thank you also to Grant McClelland for agreeing to act on my committee during the defence.

Thank you to my collaborators: the Vitkin lab at University of Toronto (MaRS), particularly Valentin Demidov and Blake Jones for their assistance with the OCT analysis. The Cranston lab in Engineering, particularly Heera Marway, and the Biointerfaces staff, particularly Elna Luckham, for their support during the development of the atomic force microscopy protocol. Thank you also to Alan Tang for his troubleshooting help.

I would also like to thank Jacobs lab members, both past and present. Thank you to Duygu and Chris for making the lab a welcoming environment when I first arrived. Your offer of chocolate the day I met you both rid me of any doubts I may have had about starting graduate school. Thank you also to Sam for her help reintroducing Western blots to the lab. It would have been a far more painful process without you! Thank you to Mihaela for her help getting the Westerns off the ground and for letting me vent when they didn't work. To all of our undergraduate volunteers and thesis students, including Runyang, Courtney, and Mae, thank you for helping to fill up the lab and for helping us keep everything running smoothly (for the most part).

Thank you to Danielle and Katie, who started this with me. Thank you to both of you for feeding Luna when I'm out of town – it makes a huge difference to know you have people you can rely on when you move to a new city. Thank you to Danielle for her uncanny ability to sense when it's time to say we need a drink, and for always making sure the lab is kept running. I swear I'll be in early enough to make fly food one of these days. Katie for her R “expertise” - you're right, it was the easier way to make a histogram. Thank you also to Katie for answering my panicked phone calls early in the morning when my laptop wouldn't turn on and I had a deadline. I owe you big time.

Finally, one last big thank you to my friends and family, who have supported me through the good and the bad. I know a lot of you find my enthusiasm for an insect to be a bit odd but thank you for encouraging me anyway.

## Table of Contents

<b>Title page</b> .....	i
<b>Descriptive note</b> .....	ii
<b>Abstract</b> .....	iii
<b>Acknowledgements</b> .....	iv
<b>Table of Contents</b> .....	vi
<b>List of figures</b> .....	viii
<b>List of tables</b> .....	viii
<b>List of abbreviations</b> .....	ix
<b>1. Introduction</b>	
1.1 The heart.....	1
1.1.1 The ECM and its importance to heart function.....	2
1.2 Cardiovascular disease.....	7
1.2.1 The ECM and cardiovascular disease.....	9
1.3 <i>Drosophila</i> model.....	12
1.3.1 The <i>Drosophila</i> dorsal vessel.....	12
1.3.2 <i>Drosophila</i> specific cardiac ECM.....	14
1.4 System for perturbing the ECM.....	15
1.5 Biophysical tools.....	19
1.5.1 Atomic force microscopy.....	19
1.5.2 Current uses for AFM in biology.....	20
1.6 Research question.....	23
<b>2. Methods</b>	
2.1 Fly stocks and crosses.....	24
2.1.1 Generating giants.....	25
2.2 Immunolabelling and Confocal Microscopy.....	25
2.2.1 Larval dissections (standard).....	25
2.2.2 Immunolabelling.....	26
2.2.3 Confocal microscopy.....	29
2.3 Body size, heart size, mass measurements.....	29
2.4 OCT imaging.....	30
2.4.1 OCT analysis.....	31
2.5 AFM protocol.....	32
2.5.1 Larval dissections for AFM analysis.....	32
2.5.2 AFM setup.....	34
2.6 Western blots.....	35
2.6.1 Western blot solutions.....	35
2.6.2 General Western blot protocol.....	36

2.6.3 Westerns run.....	37
<b>3. Results</b>	
3.1 Generating and Characterising Giant Larvae.....	39
3.1.1 Generating giant larvae.....	39
3.1.2 Body size and mass measurements.....	42
3.1.3 Core ECM component analysis.....	45
3.1.4 F-CHP in an invertebrate model.....	50
3.1.5 Functional analysis using OCT.....	52
3.1.6 Western blot of Pericardin.....	58
3.2 Atomic force microscopy protocol development.....	60
3.2.1 Selecting an appropriate AFM.....	60
3.2.2 Dissection protocol.....	63
3.3.3 Placing AFM probe on heart.....	64
3.3.4 Collecting meaningful data.....	64
<b>4. Discussion</b>	
4.1 Characterising giant larvae.....	66
4.2 Biophysical analysis of <i>Drosophila</i> tissue.....	71
4.2.1 Alternative methods of biophysical analysis.....	72
4.3 Applications of a larval obesity model.....	72
4.3.1 Further characterisation of giant larvae.....	72
4.3.2 Applications of biophysical techniques in <i>Drosophila</i> heart..	74
4.3.3 Potential applications of larval overgrowth model.....	75
4.4 Concluding thoughts.....	75
<b>5. References.....</b>	<b>77</b>
<b>6. Supplemental figures.....</b>	<b>81</b>

## List of Figures

1.1 The Extracellular Matrix.....	5
1.2 The <i>Drosophila</i> heart.....	13
1.3 Life cycle of giant larvae.....	18
1.4 Atomic force microscopy.....	21
1.5 Cross section of <i>Drosophila</i> heart with AFM probe.....	22
3.1 Size comparison of giant larvae and genetic controls.....	41
3.2 Giant larval size and mass measurements.....	43
3.3 Fatty heart phenotype in giant larvae.....	44
3.4 Confocal analysis of ECM network.....	47-48
3.5 Pericardin fibre thickness.....	49
3.6 3-Helix denatured Collagen marker in an invertebrate model.....	51
3.7 Stills from OCT videos.....	54
3.8 Contraction cycles in one plane.....	55
3.9 Lumen area and stroke volume measurements obtained using OCT.....	56
3.10 Heart rate and rhythmicity of giant and wildtype hearts.....	57
3.11 Western showing Pericardin levels.....	59
3.12 Bioscope Catalyst.....	62
S1 Westerns of individual larvae.....	81-82

## List of Tables

2.1 <i>Drosophila</i> stocks.....	24
2.2 Antibodies used for immunohistochemistry.....	28
2.3 Antibodies used for Western blots.....	38

## List of Abbreviations

AFM	Atomic force microscopy
BMI	Body mass index
<i>da</i>	<i>daughterless</i>
Dcr	Dicer
DSHB	Developmental studies hybridoma bank
DTT	dithiothreitol
ECM	Extracellular matrix
F-CHP	5-FAM conjugated Collagen hybridizing peptide (for denatured Collagen)
Hz	Hertz
Loh	Lonely heart
LOX	Lysyl Oxidase
MMP	Matrix metalloproteinase
NGS	Normal goat serum
OCT	Optical coherence tomography
PBS	Phosphate buffered saline
PBST	Phosphate buffered saline with 0.3% Triton-X-100
<i>phm</i>	<i>phantom</i>
Prc	Pericardin
SDS	SDS – sodium dodecyl sulfate
<i>sna</i>	<i>snail</i>
SPARC	Secreted protein acidic and rich in cysteine
TGS	tris, glycine, and SDS (Western running buffer)
TIMP	Tissue inhibitor of matrix metalloproteinase
Vkg	Viking
<i>yw</i>	<i>yellow white</i>

## **1. Introduction**

### **1.1 The heart**

The heart is a muscular organ, with the vital role in vertebrates of delivering oxygenated blood to the tissues of the body. The human heart is a multichambered organ that contracts in response to electrical impulses generated by the sinoatrial and atrioventricular nodes (Shih, 1994). These signals are conducted through the tissue by specialized muscle fibres, called the bundle of His (Alanis et al, 1958). The generation and timing of electrical impulses in the heart is tightly controlled, as well as their propagation through the tissue. The muscle of the heart is specialized to allow for the swift conduction of electrical signals – the fibres possess intercalated discs, a unique feature of cardiac muscles (Walker and Spinale, 1999). These discs allow for rapid transmission of electrical impulses through a tissue. Additionally, cardiac muscle is branched, creating an increased number of contacts between muscle cells.

There are two main groups of cells present in heart tissue: contractile cardiac myocytes, and fibroblasts. Myocytes perform the contractile action of the heartbeat and are supported in this role by fibroblasts (Fan et al, 2012).

Unlike the majority of muscles, the heart must contract continually throughout the life of the organism. In order to withstand the enormous amount of strain generated by continuous contractions, the tissue making up the heart is highly specialized. In part, this level of specialization is achieved by a unique extracellular matrix (ECM) (Rotstein et al, 2018). The ECM is a key modulator of cardiac function – it must be robust to withstand the constant contractile force of the heartbeat, as well as elastic enough to allow these

continual contractions. In this thesis, I will consider insights from both vertebrate and invertebrate genetic models in order to address questions in a *Drosophila* model.

### **1.1.1 The ECM and its importance to heart function**

The extracellular matrix (ECM) is a scaffold of proteins, glycoproteins and proteoglycans that are found outside of the cell membrane, and is responsible for supporting tissues, allowing for their proper function (Hughes and Jacobs, 2017). The ECM is also involved in facilitating cell-cell interactions, sequestering growth signals or other signalling factors, and influencing signal transduction (Wilmes et al, 2018). In the heart specifically, it also mediates the conduction of electrical signals (Travers et al, 2016). The makeup of the ECM is tissue specific, as the ECM must be able to support the mechanical and physiological roles of a tissue, and these roles are variable from tissue to tissue (Rotstein et al, 2018). For example, the ECM of a tendon is required to have immense tensile strength in one plane, while the ECM surrounding a neuron may act to control its growth (Mouw et al, 2014). This leads to an incredibly complex and variable ECM makeup across tissues and organ systems. This variability is accomplished by the use of different protein family members in different tissues, varying the abundance of one protein or another, and varying the amount of cross linking between the various proteins making up the matrix (Mouw et al, 2014).

In general, the ECM is composed of two distinct domains: the basement membrane and the interstitial matrix (Hughes and Jacobs, 2017; Fan et al, 2014). The basement membrane is found directly adjacent to the cell wall and is in close association with the cells and tissue, while the interstitial matrix is found further beyond the cell. The

basement membrane often acts to anchor the cell to the interstitial matrix (Walker and Spinale, 1999). Both domains are composed primarily of various forms of Collagen, with the predominant form of Collagen depending on the location. The interstitial matrix consists of mainly fibrous Collagens; the majority is Collagen I, with some Collagen III, whereas the basement membrane is primarily a network of Collagen IV (Jourdan-LeSaux et al, 2010; Lebleu et al, 2007). I will focus primarily on the basement membrane.

ECM assembly in the basement membrane is likely to follow a specific series of steps (Hollfelder et al, 2014). Cell surface receptors such as Integrin and Dystroglycan are able to recruit Laminin and Collagen to the cell surface. Laminin then forms a sheet over the surface, where it recruits Collagens. In the basement membrane, it recruits Collagen IV (shown in figure 1.1). Collagen IV binds to Laminin and is able to form a complex network across the surface of the tissue. Nidogen and Perlecan (Trol) are proteoglycans that help to stabilize the Collagen and Laminin networks (Hollfelder et al, 2014). Vertebrates also possess Fibronectin, an additional core ECM component not found in invertebrates. Fibronectin is a glycoprotein that has an Integrin binding domain and acts to crosslink and stabilize the matrix (Jourdan-LeSaux et al, 2010).

Additional stability of the matrix comes in the form of Collagen crosslinking. This is carried out by Lysyl Oxidase (LOX) and lends strength and stiffness to the matrix (El Hajj, El Hajj et al, 2018). Crosslinking of Collagen fibres also makes them more resistant to degradation (El Hajj, El Hajj et al, 2018). All of the steps outlined are required to establish the basic ECM network.

The ECM is not an inert scaffold and relies on remodelling to perform its role. The level of activity of the heart requires a matrix that is able to support this constant

motion, as well as one that is able to adapt to changing environmental conditions in order to maintain organ function (Rotstein et al, 2018; Hollfelder et al, 2014). Due to the requirements of this system, the cardiac ECM is highly regulated and is implicated in the majority of diseases affecting the heart (Travers et al, 2016).

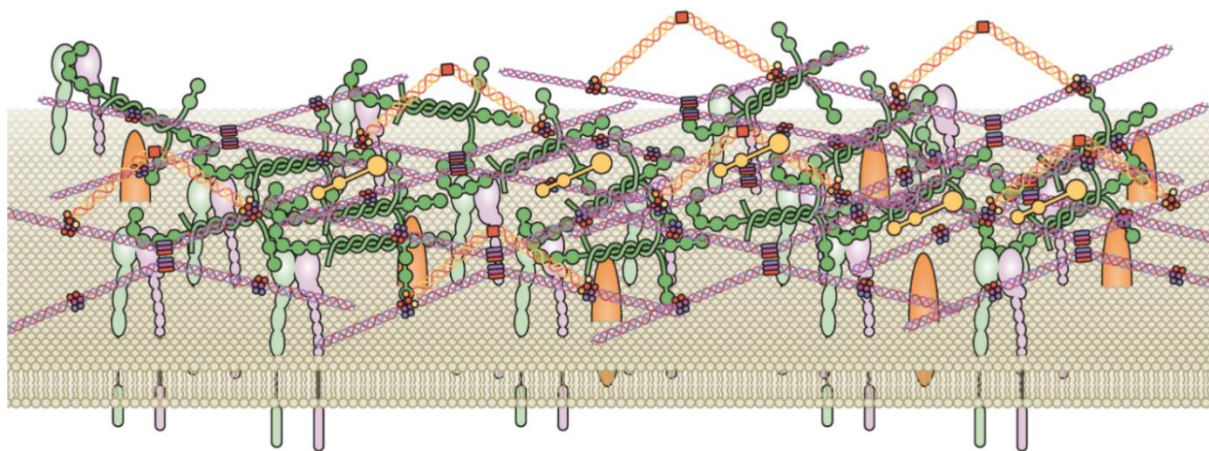


### Figure 1.1: The Extracellular Matrix

Structure of the ECM, showing Integrin (embedded in the cell membrane, light green and light purple) and Dystroglycan (embedded in cell membrane, orange) binding to Laminin (dark green). Laminin is able to form a sheet over the cell membrane, where it is then able to recruit Collagens (purple and orange). Nidogen (yellow) facilitates the binding of Laminin and Collagen. Once Collagen is recruited to the matrix, it forms a complex network. (Adapted from Mouw et al.)

Remodelling of the ECM is a normal process involving protein turnover, deposition, and crosslinking that is necessary for the maintenance of tissue function (Bogatan et al, 2015; Hughes and Jacobs, 2017). The protein deposition involved in remodelling is precisely controlled, both temporarily and spatially, in order to preserve the functionality of the ECM (Rotstein et al, 2018). ECM remodelling is also critical for facilitating tissue growth, particularly during development (Mouw et al, 2014). In *Drosophila*, knockdown of heart specific Collagen or its receptor causes complete collapse of the heart tube, and dissociation of the pericardial cells and alary muscles (Rotstein et al, 2018), while Laminin B1 mutants also display dissociation of the pericardial cells and alary muscles from the heart tube (Hollfelder et al, 2014). A  $\beta$ 1-Integrin knockout is embryonic lethal in mice, while those that are heterozygous for the knockout display impaired heart function and intolerance to cardiac stress (Shai et al, 2002). These examples highlight the importance of a functional, appropriately structured matrix to heart development and function.

Remodelling is accomplished by a family of proteins called the matrix metalloproteinases (MMPs), and their inhibitors, tissue inhibitor of metalloproteinase (TIMPs) (Hughes and Jacobs, 2017). MMPs are responsible for the breakdown of various ECM components, including Collagen. The levels of MMPs in a system are regulated by TIMPs at the post-translational level. The levels of MMPs and TIMPs in a tissue establish a balance of protein deposition and breakdown within a healthy ECM (El Hajj, El Hajj et al, 2018).

## 1.2 Cardiovascular disease

The heart is a highly specialized organ and requires a great deal of control to maintain its performance over the life of an organism. Due to the complexity in this system, there are multiple ways to challenge cardiac function, and various diseases that can affect the heart. These diseases all fall into the category of cardiovascular disease, a range of conditions that result in impaired cardiac function (Travers et al, 2016). The term cardiovascular disease has a wide variety of meanings, from a sudden, acute disease state as occurs in myocardial infarction, to chronic, progressive conditions, that eventually lead to heart failure (Jourdan-LeSaux, 2010; Travers et al, 2016). There are many causes of cardiovascular disease, from congenital defects to lifestyle habits. Despite the range in causes, there are several defining characteristics of heart disease. Pathological remodelling of the heart tissue, or fibrosis, is present in the majority of cases of cardiovascular disease (Travers et al, 2016). Fibrotic remodelling is caused by increased deposition of the extracellular matrix by cardiac fibroblasts, as well as increased cross-linking of ECM components (Meschiari et al, 2017).

The heart has limited capacity to regenerate after injury and relies mainly on tissue remodelling to repair damage caused by a disease state (Travers et al, 2016). Remodelling leads to changes to the heart architecture, including replacement of damaged muscle tissue with connective tissue. This can result in heavily scarred, non-contractile heart tissue as heart failure progresses (Travers et al, 2016). Initially, this remodelling is adaptive in a disease state in order to maintain heart integrity but is maladaptive for optimal heart function. Cardiovascular disease often causes the death of myocytes, leaving gaps in the tissue that are weaker than the surrounding tissue. These

areas are at risk of rupture as the heart continues to contract (Travers et al, 2016; Jourdan-LeSaux et al, 2010). In order to ensure that these regions do not rupture and compromise the entire organ, ECM proteins are deposited to increase the strength of the damaged tissue. The result of this immediate solution is maladaptive in the long term – formation of scar tissue leads to impaired function of the heart, with the impairment growing progressively worse over time (Travers et al, 2016).

The incidence of cardiovascular disease in modern society is remarkably high. Among Canadians, cardiovascular disease as a cause of death is second in prevalence only to cancer, with approximately 1 in 12 adults affected (Government of Canada, 2017). The development of cardiovascular disease can be attributed to various risk factors, the most common of which are aging and obesity (Government of Canada, 2017; Poirier et al, 2006; Sessions et al, 2017). Current rates of obesity are extremely high, with approximately 1 in 4 Canadian adults having a body mass index (BMI) above 30, which classifies them as obese (Statistics Canada, 2018). An additional 1 in 3 have a BMI above 25, categorizing them as overweight. This leaves only 40% of Canadian adults with what is considered a healthy weight (Statistics Canada, 2018). With the addition of an aging population, this puts a large percentage of Canadian adults at risk of developing cardiovascular disease in their lifetime. This makes the study of cardiovascular disease and its risk factors of critical importance.

### 1.2.1 The ECM and cardiovascular disease

Regulation of the ECM, particularly of the process of remodelling, must be tightly controlled to support tissue function. To maintain the role of the cardiac ECM as a key modulator of heart function, this high level of regulation is used to control the balance of protein breakdown and deposition in the tissue. When this balance is disrupted, changes to the mechanical properties of the system occur (Jourdan-LeSaux et al, 2010). As stated previously, aberrant or excessive ECM remodelling can be triggered in response to environmental stimuli, such as those present in cardiovascular disease states, leading to fibrosis (Jourdan-LeSaux et al, 2010).

Disease states are not the only cause of fibrosis. Fibrosis is also known to occur with aging as a result of the age-related accumulation of reactive oxygen species, and dysregulation of the immune response (Cieslik et al, 2011). Lifespan in *Drosophila* can be improved by reduction of Integrin levels (Bogatan et al, 2015) as well as knockdowns of the ECM components Laminin A, Pericardin, and Viking (Sessions et al, 2017). By reducing the amount of fibrotic tissue in the system, tissue function is maintained, and lifespan is increased, demonstrating the importance of the ECM to overall health. While both aging and disease can contribute to the development of fibrosis, I will focus on disease.

In the context of cardiovascular disease, remodelling can be triggered by a variety of factors, including acute tissue injury as a result of blood clots or plaque build up, impaired blood flow due to vascular blockages or constriction, or as a result of chronic overload and the resulting cardiac stress. These all cause apoptosis and necrosis of myocytes within the tissue. Upon their death, these cells release reactive oxygen species

and other signalling factors, which induce the expression of NF- $\kappa$ B. This in turn upregulates pro-inflammatory cytokines and activates an inflammatory response within the tissue (Travers et al, 2016; Jourdan-LeSaux et al, 2010). Inflammation signals to immune cells to invade the tissue to begin to clear out dead matter (Jourdan-LeSaux et al, 2010). As immune cells invade, macrophages release TGF- $\beta$ 1, which causes the differentiation of fibroblasts into myofibroblasts (Jourdan-LeSaux et al, 2010; Fan et al, 2012). Myofibroblasts are only found in a tissue following an injury and produce more ECM proteins than fibroblasts (Fan et al, 2012). The conversion of fibroblasts to myofibroblasts leads to an increase in ECM protein deposition in an effort to preserve tissue functionality (Travers et al, 2016). While it is critical that these proteins be laid down as an immediate solution to a weakened area of tissue, this repair mechanism can have catastrophic consequences for tissue function after the injury. Myocytes are specialised heart cells that provide the contractile force for pumping of the heart. Additionally, the ECM normally plays a role in the conduction of electrical signals through the cardiac tissue (Travers et al, 2016). Misregulation of remodelling as is observed in disease states creates an ECM with a structure that does not support optimal tissue function. Fibrosis results in impaired heart contractility, increased stiffness of the ventricles, contractile dysfunction, and impaired conduction of electrical signals through the tissue (Jourdan-LeSaux et al, 2010; Fan et al, 2012; Travers et al, 2016).

After the ECM has been reinforced and there is no longer a risk of the heart rupturing, myofibroblasts begin to die off. However, not all myofibroblasts undergo apoptosis – a subset persists within the tissue, depositing more Collagen and other ECM

proteins than is necessary. This leads to progression of fibrosis over time and contributes to the development of heart failure (Travers et al, 2016).

Impaired cardiac function prevents the proper delivery of oxygenated blood to tissues to the body (Jourdan-LeSaux et al, 2010). The pathological processes associated with cardiac fibrosis lead to disease progression and heart failure (Travers et al, 2016). Increased levels of fibrosis are associated with poor clinical outcomes in patients with symptomatic aortic stenosis who are recovering from aortic valve replacement (Weidemann, Hermann et al, 2009). As this factor is not often taken into account prior to surgery, it helps to account for variable outcomes following this procedure. LOX inhibitors have also been shown to prevent increased levels of pro-fibrotic MMPs and TIMPs, as well as increased levels of Collagen crosslinking in ventricular overload models (El Hajj, El Hajj et al, 2018). These examples demonstrate the importance of the cardiac ECM and its remodelling in the study of cardiovascular disease.

The proteins that are involved in remodelling have been partially characterised, but this is an incredibly complex system with much genetic redundancy and high levels of variability. The cardiac ECM is critical for the health and function of the heart as a whole. Therefore, it is necessary that the regulatory mechanisms and key players involved in ECM remodelling are studied. In addition, the impact of ECM remodelling on the biophysical characteristics, such as elasticity, of a tissue is of key importance when considering the impact of cardiovascular disease on tissue function. This remains an area where little work has been done.

### **1.3 *Drosophila* model**

It is readily apparent that the changes associated with fibrosis of the heart cause catastrophic consequences to patients and their quality of life. The cardiac ECM is a complex system, possessing a great deal of genetic redundancy. This makes it difficult to determine the precise roles of various protein players in this process, as there are compensatory mechanisms. Their study requires the use of a simple model organism.

*Drosophila melanogaster* is an invaluable genetic model for the study of complex phenotypes due to its low genetic redundancy, well characterised genome, and the wide availability of molecular tools (Hughes and Jacobs, 2017). *Drosophila* is the simplest model organism that possesses a heart, and undergoes drastic morphological changes throughout its development, all of which require ECM remodelling. This makes *Drosophila* an ideal model for the study of complex cardiovascular phenomena and ECM remodelling.

#### **1.3.1 The *Drosophila* dorsal vessel**

The *Drosophila* heart, also called the dorsal vessel, is used as a model for the mammalian heart as its development closely mirrors early mammalian heart development, and the pathways involved in its formation are highly conserved (Hughes and Jacobs, 2017). The *Drosophila* heart is a long tubular structure that is made up of 52 contralateral cardioblasts that migrate towards the midline during embryogenesis and fuse to create a tube (figure 1.2). This tube is flanked by pericardial cells, which act as detoxifying nephrocytes. The heart is suspended within the body cavity and is anchored to the epidermis by 7 pairs of alary muscles (Hughes and Jacobs, 2017).

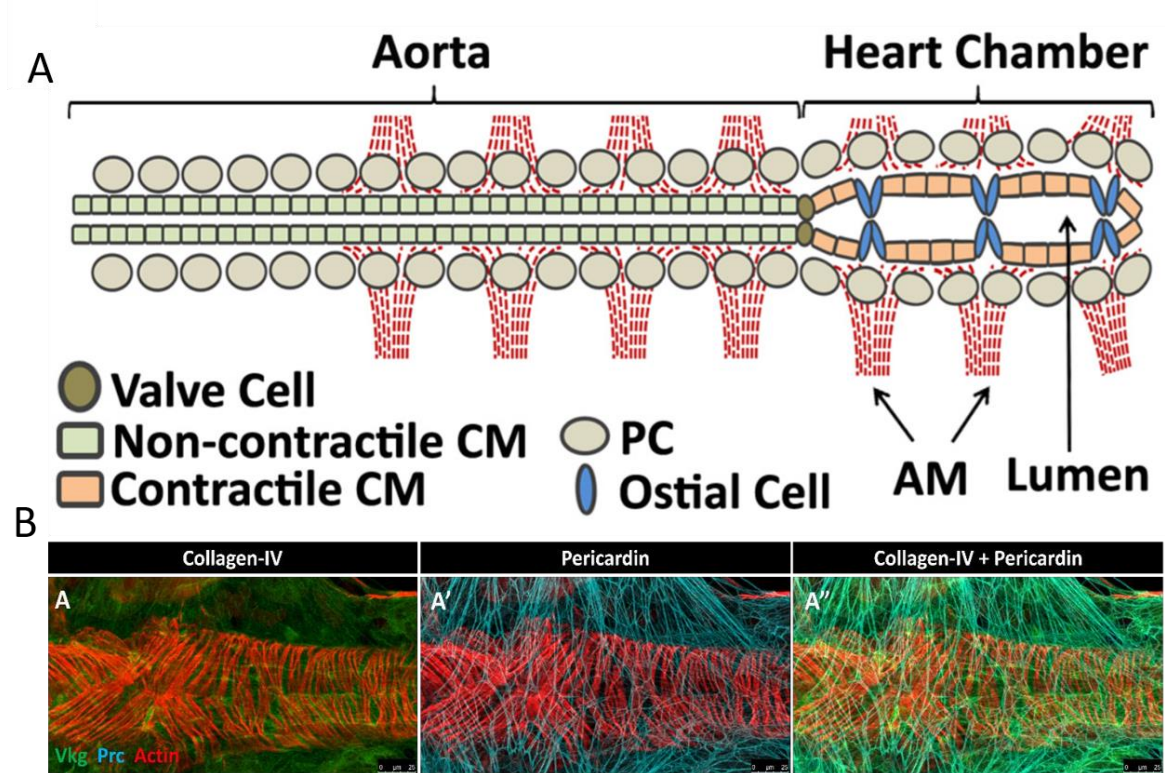


**Figure 1.2: The *Drosophila* heart**

A) Schematic of the larval *Drosophila* heart. 52 pairs of cardioblasts form the heart tube and are flanked by pericardial cells (Adapted from Hughes and Jacobs, 2017). B) The ECM network surrounding the *Drosophila* heart (Adapted from Hughes, 2018).

### 1.3.2 *Drosophila* specific cardiac ECM

The *Drosophila* cardiac ECM is made up of many of the same protein families, although with less genetic redundancy, that are also found in a mammalian system. This high degree of conservation makes the *Drosophila* heart a model system well suited to ECM research (Wilmes et al, 2018). The cardiac ECM is required to anchor the dorsal vessel within the body cavity, to help anchor the alary muscles to the heart tube, and to hold the pericardial cells in close association with the heart (Hughes and Jacobs, 2017; Hollfelder et al, 2014). The matrix consists mainly of Collagen IV (Viking) and the Collagen IV-like protein Pericardin. Pericardin (Prc) is a heart specific Collagen found in *Drosophila*.

Much like other matrices, the *Drosophila* cardiac ECM is anchored to the cell by the transmembrane receptors Integrin and Dystroglycan. Integrin is able to bind to the main network forming components of the matrix, Collagen IV and Laminin. These form a complex network which is stabilized by the binding of Nidogen and Perlecan (Trol), as well as crosslinking of the various ECM components by Lysyl Oxidase (LOX) (Hollfelder et al, 2014).

In addition to these proteins, the *Drosophila* cardiac ECM has the unique Collagen Pericardin. Prc is recruited to the heart by the ADAMTS-like protein Lonely heart (Loh). Loh is present only on the surface of the heart, where it recruits Prc (Rotstein et al, 2018). Prc is then able to incorporate into the cardiac ECM. Loh is necessary and sufficient for the recruitment of Prc to the heart, with ectopic Loh able to recruit Prc to other tissues. The incorporation of Prc into muscle ECM leads to impaired contractility of this tissue, suggesting that Prc is a highly specialized ECM component, required for the

additional strain that heart muscle faces as a result of the need for constant contractions over the life of the organism (Wilmes et al, 2018).

*Drosophila* does not possess Fibronectin, a glycoprotein that binds to Integrin and helps to crosslink and stabilize the matrix in vertebrates (Jourdan-LeSaux et al, 2010). Fibronectin is present only in vertebrates. *Drosophila* also lacks the fibroblasts present in the vertebrate heart, with the heart tube formed by cells called cardioblasts that differentiate into cardiomyocytes (Hughes and Jacobs, 2017).

Remodelling of the matrix is necessary during growth and development of the tissue, as well as to maintain tissue function during the aging process and in response to environmental stimuli. This remodelling is accomplished by a family of proteins called the matrix metalloproteinases (MMPs), and their inhibitors, tissue inhibitor of metalloproteinase (TIMPs). In *Drosophila*, there are 2 MMPs, MMP1 and MMP2, and one TIMP. MMP1 is secreted, while MMP2 is membrane bound (Hughes and Jacobs, 2017). Both are required for heart development, with MMP1 necessary for the maintenance of the lumen, and MMP2 necessary for the restriction of the luminal area (Raza et al, 2017). The regulation of ECM proteins during development by the MMPs leads to the appropriate formation of the heart tube.

#### **1.4 System for Perturbing the ECM**

There have been numerous studies in *Drosophila* where the role of the ECM during embryonic morphogenesis has been examined. These studies have discovered key components of the signalling pathways necessary for coordinated cell migration and heart formation, and the role that the ECM plays in this process (Bogatan et al, 2015;

Vanderploeg and Jacobs, 2015). In addition, studies of the cardiac ECM in adult *Drosophila* and its role in various aging phenotypes have also been examined (Sessions et al, 2017). During larval growth, the larval heart must grow to accommodate a five times increase in body size over the course of only three to four days (Bogatan et al, 2015). This massive amount of growth is accomplished with no cell division, only by tissue remodelling. Larval *Drosophila* is therefore an ideal system for studying matrix remodelling and is a system that is underutilized and understudied.

In order to examine the impact of fibrosis on cardiac function, a model for cardiovascular disease in *Drosophila* is needed. This led me to employ the use of a genetic model for obesity. By knocking down the transcription factor *snail* by RNAi mediated depletion of the transcript in the prothoracic gland, the ecdysone pulse required for control of the critical weight checkpoint and entry into pupation is eliminated (Zeng, 2017) This causes a developmental arrest, and locks larvae in a state of perpetual growth (figure 1.3). The resulting giant larva phenotype has been noted as a side effect of hormonal manipulations with *Drosophila* larvae, particularly in studies looking at steroid hormone synthesis (Zeng, 2017). While it was noted that this phenotype was an indication that normal developmental regulation had been disrupted, it was not utilized as a model in its own right. I will employ this giant larval phenotype as a model for obesity and cardiovascular disease in *Drosophila* in order to observe the impact of increased body size on the *Drosophila* heart.

Other systems to produce obesity in *Drosophila* have been employed, including diet induced models as well as manipulations to the Insulin signalling pathway. Diet induced models involve supplementing standard fly media with a source of fat, such as

coconut oil (Diop et al, 2017). Coconut oil feeding has been used in studies of the adult *Drosophila* heart to determine the impact of a high fat diet on heart function (Birse et al, 2010). However, this method has not been employed in larvae, and only transiently in adults.

Insulin signalling is involved in the same hormone synthesis pathways that are altered in giant larvae. Insulin signalling mutants display reduced body size, while insulin overexpression results in significantly increased body size (Oldham et al, 2002). An increase in adult body size of approximately 40% was observed in adult flies with ubiquitous insulin overexpression, as a result of both cell growth and proliferation (Brogiolo et al, 2001). This system has only been utilized to observe size differences in adult flies and does not yield an increase in body size as extensive as the giant larval model (Zeng, 2017).

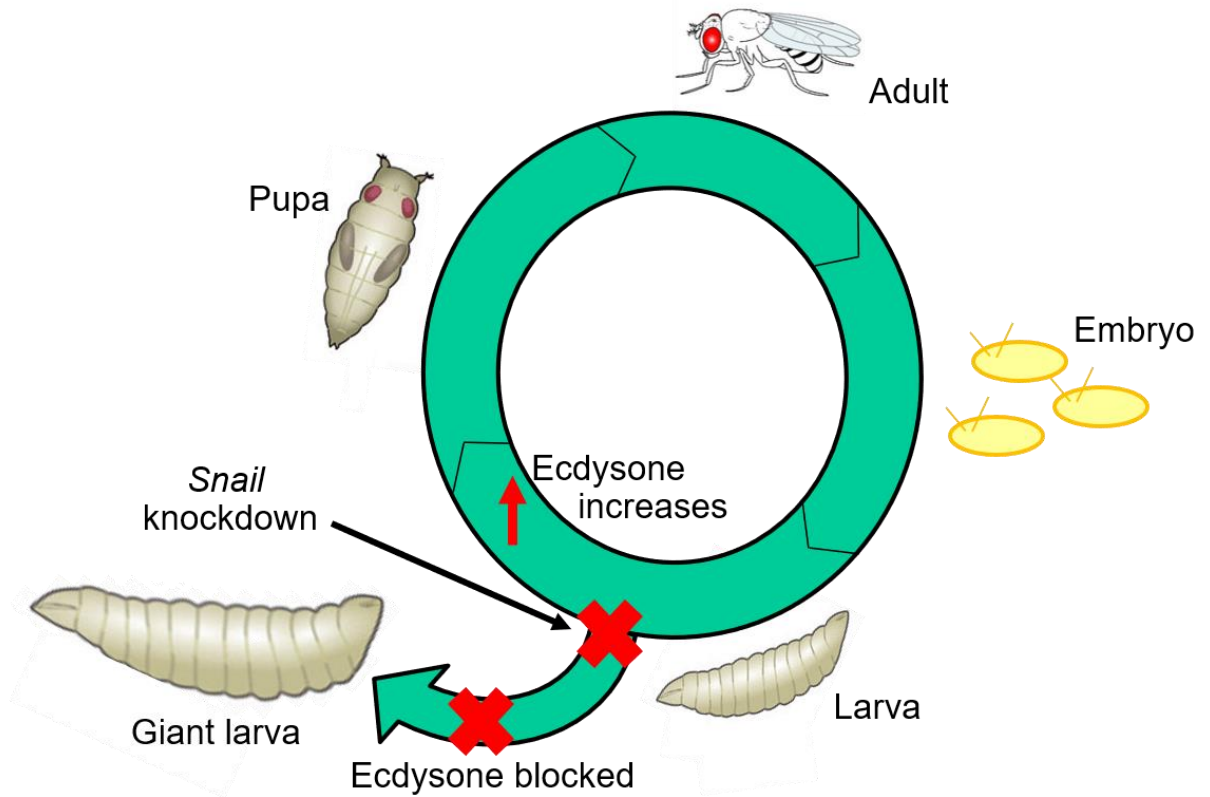


**Figure 1.3: Life cycle of giant larvae**

In wildtype organisms a pulse of ecdysone in late larval stages is the signal for the larva to pupate. By knocking down the transcription factor *snail* this pulse is prevented, locking larvae in a state of perpetual growth.

## **1.5 Biophysical tools**

Biophysical characteristics of a tissue, including elasticity and tension, are important for its proper function. Although important, these characteristics are typically not studied in living systems. The only methods used to study the ECM and its regulation are indirect. A Western blot may be used to examine protein abundance, or immunohistochemistry may be used to study protein distribution. Measures of cardiac function, such as cardiac output and contractility, can be obtained from live imaging. While these measurements are informative, there is a gap in our understanding of how the biophysical characteristics of the ECM play a role in the overall function of a tissue. In order to take measurements of the biophysical properties of a system, methods outside of these classical molecular assays are required.

Atomic force microscopy (AFM) is a method by which a probe is placed directly on a surface. The physical contact between probe and sample allows for direct measurements of tissue properties, unlike conventional assays (Kirmizis and Logothetidis, 2010). This allows for the quantification of factors such as tissue elasticity that are not possible to measure simply by observation.

### **1.5.1 Atomic force microscopy**

Atomic force microscopy (AFM) is a technique that is underutilized in biological sciences. In this technique, a probe on a flexible cantilever is placed in direct contact with a surface. A laser is aimed at the cantilever and the reflected laser light is picked up by a photodetector (figure 1.4). This allows for tracking of the probe as it moves across the surface and can be used to generate detailed surface topography images at a nanoscale

(Kirmizis and Logothetidis, 2010). Another application of this is to measure how much force is required to indent the probe a set distance into a sample. This generates a force curve for a given point. By measuring force curves across a sample, general information about elasticity and tension (“stiffness”) can be acquired (Kirmizis and Logothetidis, 2010). When applied to a tissue sample, this can yield invaluable data regarding ECM characteristics that cannot be obtained without the direct contact between probe and sample found in AFM.

### **1.5.2 Current uses for AFM in biology**

AFM has been used on tissue preparations as a way to measure tissue stiffness, particularly in cell migration models (Kim et al, 2014; Chen et al, 2018). In mammalian models, AFM has been used to measure the stiffness of developing cartilage in order to assess the impact of gene knockdowns (Xin et al, 2016). AFM is also somewhat commonly used in cell culture. It has been used in the *Drosophila* optic stalk to correlate tissue stiffness and cell migration (Kim et al, 2014), as well as in the *Drosophila* brain to measure the impact of a Piezo1 knockdown on a glioma model (Chen et al, 2018). These applications allow for the tissue to be removed from the body of the organism and studied separately. However, the *Drosophila* heart is suspended in the middle of the body cavity and its removal would cause massive damage to the cardiac ECM. In order to measure the characteristics of the ECM in this tissue, it is necessary to apply AFM to an *in situ* tissue preparation (figure 1.5). This is a novel application of this technique and has the potential to revolutionize the study of protein dynamics in a living system.

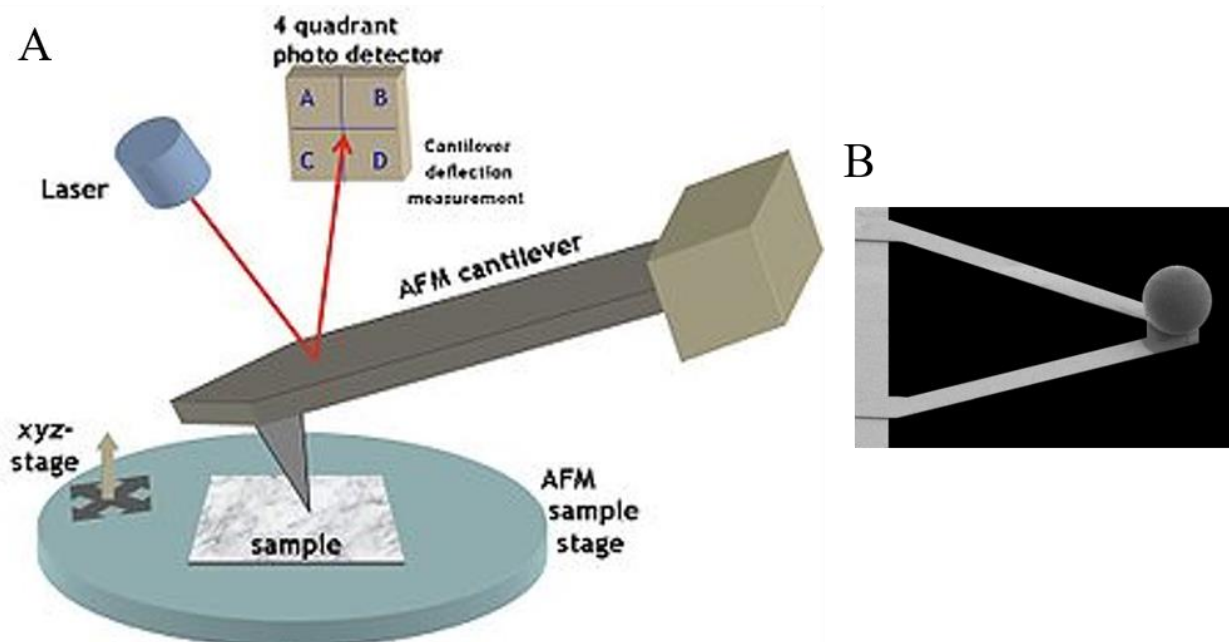


#### Figure 1.4: Atomic force microscopy

A) A schematic of the basic AFM setup. A probe is mounted on a flexible cantilever, with a laser trained on it. Laser light is detected by a photodetector and is able to track surface topography or determine when a trigger point is reached. B) Colloidal probes consist of a spherical probe mounted on a flexible cantilever and are typically used for biological applications. (A adapted from the Opensource Handbook of Nanoscience and Nanotechnology. B adapted from AppNano AFM probes.)

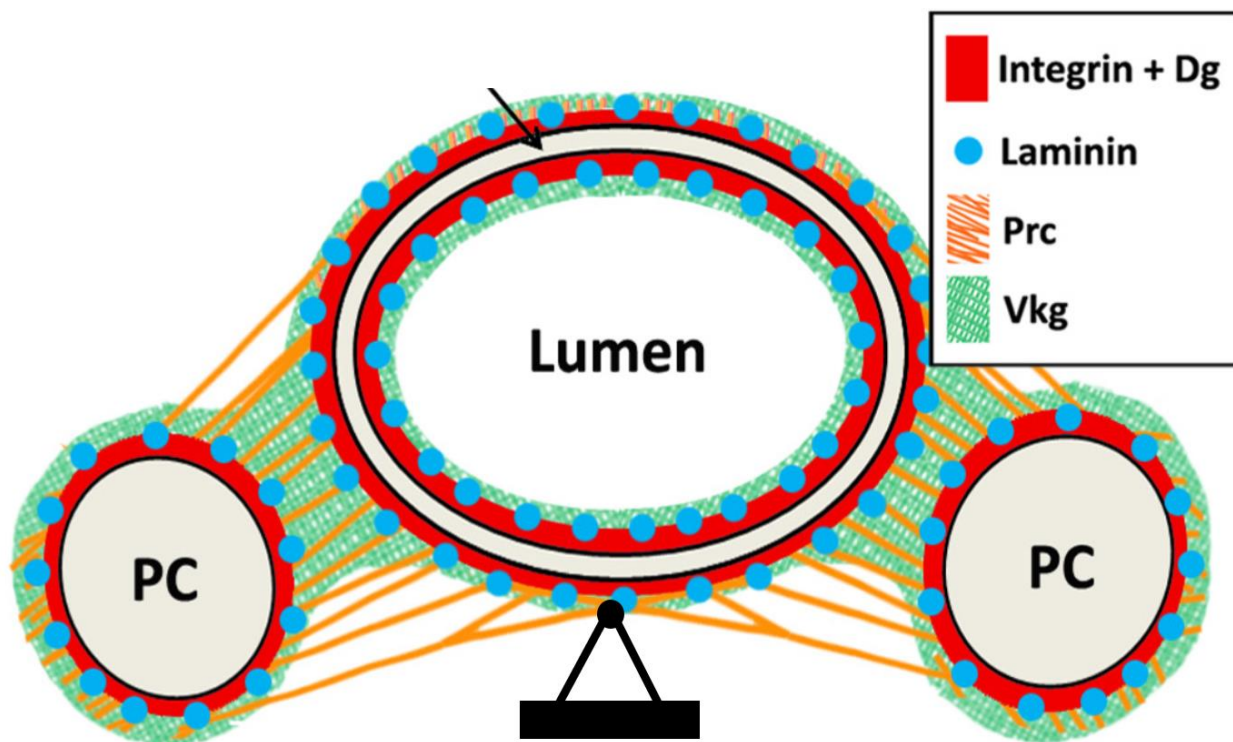


**Figure 1.5: Cross section of *Drosophila* heart with AFM probe**

AFM probe (not to scale) shown in black at the bottom of a larval heart cross section. The dorsally positioned heart is accessed through ventral dissection. The probe is then lowered onto the sample and makes measurements of tissue characteristics by recording force curves for points along the surface.

PC = pericardial cell (Adapted from Hughes and Jacobs, 2017).

## 1.6 Research question

Using my genetic model for obesity, I aimed to characterise the impact of a large body size on the heart of *Drosophila melanogaster*. Using classical molecular biology assays, including Western blot, and immunohistochemistry followed by confocal microscopy, I examined the impact of body size on matrix composition and turnover. I also performed live imaging using optical coherence tomography (OCT) to examine the functional impact of obesity on luminal architecture, stroke volume, and rhythmicity. In addition, I developed a protocol for the novel use of atomic force microscopy to measure elasticity of the cardiac ECM *in situ*. Through the applications of these techniques to my larval overgrowth model, I will characterise a model for aberrant ECM remodelling that will allow for experiments that attempt to rescue a fibrosis phenotype.

## 2. Methods

### 2.1 Fly stocks and crosses

Stock	Information	Chromosome	Source
sna50003	RNAi for <i>snail</i>	X	VDRC
sna50004	RNAi for <i>snail</i>	X	VDRC
phm22Gal4	Prothoracic gland driver	III	Michael B. O'Connor
<i>UAS-Dicer2;Pin/CyO</i>	Dicer	X	Bloomington (24644)
<i>UAS-Dicer2,mCherry/CyO</i>	Dicer	II	Bloomington (59022)
<i>y<sup>1</sup>w<sup>1118</sup></i>	<i>yw</i>	X	Bloomington (6598)
<i>daGal4/Tm6-GFP</i>	Ubiquitous driver	III	This lab
<i>y[1]v[1]; P{y[+t7.7]v[+t1.8]=TRiP.JF03094}attp2</i>	RNAi for <i>snail</i>	III	Bloomington (28679)
<i>UAS-GFP/CyO-GFP;Phmgal4</i>	Prothoracic gland driver		Bloomington (26159)
<i>Fm7-GFP</i>	Fm7 balancer	X	Bloomington (5193)
<i>sna50003,UAS-Dicer2/Fm7-GFP</i>	RNAi for <i>snail</i> with <i>Dicer</i>	X	This thesis

**Table 2.1: *Drosophila* stocks**

All stocks were maintained at room temperature.

For most experiments, the following crosses were performed:

- 1) *sna50003,UAS-Dcr2/Fm7* ♀ x *phm22Gal4* ♂ → *sna50003,UAS-Dcr2;phm22Gal4*
- 2) *sna50003,UAS-Dcr2/Fm7* ♀ x *yw* ♂ → *sna50003,UAS-Dcr2/+*
- 3) *phm22Gal4* ♀ x *yw* ♂ → *phm22Gal4/+*

Crosses were performed at 25<sup>0</sup>C. Cross 1) yielded giant larvae, while crosses 2) and 3) yielded genetic controls.

For OCT analysis and 3-Helix denatured Collagen marker trials, WT larvae were used as a control. These larvae had the genotype *yw*. For immunolabelling and Western blots, giant larvae were compared to genetic controls.

### 2.1.1 Generating giants

Recombination was performed to obtain flies with the genotype *sna50003,UAS-Dcr2/Fm7*. This stock can be crossed to the prothoracic driver *phantom22Gal4* at 25<sup>0</sup>C to successfully obtain giant larvae. When this cross is performed at temperatures above 28<sup>0</sup>C, lethality results.

## 2.2 Immunolabelling and Confocal Microscopy

### 2.2.1 Larval dissections (standard)

Larval dissections are performed following the protocol outlined in Brent et al (2009). Larvae are placed on a glass plate with a well in the centre. Larvae are placed in this well and restrained dorsal side down using pins. The well is filled with 1xPBS buffer and an incision is made in the cuticle of the larva. The incision is made down the centre of the ventral side. Once the incision is made, the cuticle is pinned back, and the internal organs and fat bodies of the larva are removed using No.5 forceps and microdissection

scissors. This exposes the heart and the trachea of the larva. Trachea can be removed if they obstruct the heart. The larva is fixed using 4% paraformaldehyde fixative for five minutes on the dissection plate before being transferred to a well plate where fixation is completed. If more than one dissection is being performed, the well plate is kept on ice until all dissections are complete. Once all specimens have been dissected, the well plate is removed from ice and fixation is completed at room temperature.

### **2.2.2 Immunolabelling**

After dissection, larval specimens are fixed at room temperature for 20 minutes without shaking. After 20 minutes, the fixative is removed, and larvae are washed in 1xPBST for 3x10 minutes at room temperature with shaking. After washes, specimens are blocked in 150 $\mu$ L of 1xPBST with 10 $\mu$ L of normal goat serum (NGS) for 20-30 minutes at room temperature with shaking. Blocking solution is then removed, and primary antibody solution is added (5 $\mu$ L of each antibody in 150 $\mu$ L of 1xPBST). Specimens are incubated with primary antibody solution overnight at 4<sup>0</sup>C, with shaking. Following the primary antibody labelling, specimens are washed for 3x10 minutes with shaking at room temperature in 1xPBST. Secondary antibody solution can then be added (1 $\mu$ L of each antibody in 150 $\mu$ L of 1xPBST). 2 $\mu$ L of phalloidin can be added to the secondary antibody solution if being used. Incubate for one hour at room temperature with shaking. Remove secondary antibody solution after one hour and wash 3x10 minutes in 1xPBST at room temperature with shaking. An additional ten minute wash is completed after this using 1xPBS to remove any Triton-X-100 from the specimens. After the final wash 1xPBS is removed and 50% glycerol is added. Store at 4<sup>0</sup>C (no shaking)

for at least 3 hours. Remove 50% glycerol and replace with 70% glycerol. Specimens should remain in 70% glycerol overnight, at 4<sup>0</sup>C.

**Modifications for F-CHP denatured Collagen marker:** Specimens were fixed for 20 minutes at room temperature, then washed for ten minutes in 1xPBST three times.

Blocking was performed for 20-30 minutes in 150 $\mu$ L of PBST and 10 $\mu$ L of normal goat serum. Following blocking, specimens were labelled with 647 phalloidin (2 $\mu$ L in 150 $\mu$ L of 1xPBST) at room temperature for one hour with shaking. Two ten-minute washes were then performed. 80 $\mu$ L of F-CHP marker was added to 120 $\mu$ L of 1xPBST (final concentration of 20 $\mu$ M) and incubated overnight at 4<sup>0</sup>C, with shaking. Three ten-minute washes in 1xPBST were then performed, followed by one ten-minute wash in 1xPBS. Specimens were then placed in 50% glycerol for at least three hours, then in 70% glycerol overnight at 4<sup>0</sup>C.

1 <sup>0</sup> antibody/ conjugated marker	Concentration used at (from stock solution)	Supplier	2 <sup>0</sup> used
Pericardin	1/30	DSHB (EC11)	Alexa 488 $\alpha$ -mouse
Integrin ( $\beta$ PS)	1/30	DSHB (CF.6G11)	Alexa 488 $\alpha$ -mouse
Viking	1/30	Creative Laboratory Ltd	Alexa 488 $\alpha$ -mouse
F-CHP	20 $\mu$ M	3-Helix	N/A
647 Phalloidin	1/75	Thermofisher	N/A

**Table 2.2: Antibodies used for immunohistochemistry**

All antibodies were diluted in 1xPBST. 647 Phalloidin was added at the same time as secondary antibodies. All secondary antibodies ordered through Thermofisher and used at 1 in 150.

### 2.2.3 Confocal microscopy

Immunolabelled specimens were examined using a Leica SP5 confocal microscope. Integrin, Viking, and the F-CHP denatured Collagen marker were imaged at 20 times magnification. Pericardin was imaged at 20 times magnification to obtain images of the whole heart, and 63 times magnification with 4 times zoom to examine Pericardin fibre thickness. All images were acquired using a 60 $\mu$ m pinhole at 400Hz. Laser power was not standard across all images as lasers were replaced midway through data collection. All images are projections of z-stacks and were processed using ImageJ.

**Pericardin fibre thickness measurements:** Projections of z-stacks taken at 63 times magnification with 4 times zoom were used. A transect was drawn across the length of the image, and all fibres crossing the transect were measured. This was performed for one larva of each of the following genotypes: *snail*/+, *phantom*/+, *giant*.

### 2.3 Body size, heart size, mass measurements

When dissections were performed, images were taken of the whole body of the larva, and the width of the heart tube. Some larvae also had images taken of the length of the heart chamber. Images were obtained using a Moticam MP 3.0. An image of a micrometer was taken at the same magnification as the images of the larvae and their hearts to obtain a scale. Larvae were then measured from these images using ImageJ and the scale from the micrometer. Measurements of the length and width of the larval body were obtained, as well as measurements of heart diameter. In some cases, length of the heart chamber was also measured.

To measure the mass of individual larvae, a Mettler Toledo Microbalance (XPE56/XPE26) was used. Individual larvae were rinsed in 1xPBS and rolled on a Kimwipe to dry. The microbalance was tared between each measurement. All mass measurements were obtained in milligrams. After being weighed, larvae were either flash frozen in liquid nitrogen for use in Western blots or dissected and immunolabelled.

Unpaired t-tests were performed using graphpad.com on all larval size, heart width, and mass measurements. A Bonferroni correction was applied to all p-values (Gaetano, 2013). P values listed in results are corrected values.

#### **2.4 OCT imaging**

Performed in the lab of Alex Vitkin at the University of Toronto (MaRS) with assistance of Valentin Demidov and Blake Jones. Data was collected in the manner outlined in Bogatan et al (2015).

Specimens were oriented dorsal side up on a microscope slide coated in double sided tape. Un-anesthetised specimens were stuck to tape and allowed to acclimate for approximately ten minutes before imaging. A paintbrush dipped in 1xPBS was used to prevent desiccation of specimens. A 20 second video clip of the heart beating was recorded for each larva. From this video, contraction cycle diagrams were generated. These diagrams track the apexes of the heart walls throughout the 20 second recording and allow for quantification of heart rate and rhythmicity.

### 2.4.1 OCT analysis

Various measurements were obtained from OCT videos and contraction cycle diagrams.

**From videos:** Stills were taken at diastole and systole of three different heart beats. The luminal area was then quantified using ImageJ. Luminal area was measured three times per still, and averaged. Diastole and systole measurements were averaged for each larva, and for all larva of a single genotype. These measurements were used to determine the change in area over the contraction cycle, which was used as an approximation of stroke volume.

**From contraction cycle diagrams:** Heart rate was measured by counting the number of heart beats in 20 seconds. Heart rate was recorded in Hertz (Hz). The distance between peaks in the cycle was measured and used to generate a rhythmicity index. This was calculated following the method outlined in Gomez et al (2019). In short, the average and standard deviation was calculated for each larva. The standard deviation was then divided by the average, giving a rhythmicity index.

Unpaired t-tests were calculated for all of the above measurements using graphpad.com.

## **2.5 AFM protocol**

### **2.5.1 Larval dissections for AFM analysis**

Constraints of the Bruker Bioscope Catalyst used for these experiments prevented the use of a standard dissection setup. The allowance of the AFM probe head was not enough for the use of dissection pins. The scanning head is bulky and must get close to the specimen before the probe can be lowered. Thus, the specimen must be as flat as possible. Additionally, a standard dissection plate is 75x50mm. The Bioscope catalyst is only able to accommodate a standard microscope slide, 75x25mm. Specialized dissection setups were therefore required. This led to the development of a new dissection protocol, using a standard microscope slide and tissue glue to hold the specimen in place.

AFM dissections are performed on a standard microscope slide. Prior to the dissection, a small amount of the slide is scored using a diamond pencil and removed. This is due to the constraints of the scanning head – the probe is only able to be moved small distances to position it above the heart. If the dissection is not perfectly centered on the microscope slide, the specimen will be outside of the range of the probe. When a small piece of the microscope slide is removed, the sample can be positioned within the scanning range of the probe.

Prior to dissection, larvae must be anesthetised using chloroform, as described in Cevik et al (2019). In brief, larvae are placed on a standard microscope slide. A piece of cotton is inserted into one end of a glass cylinder (open on both ends) and 500 $\mu$ L of chloroform is applied to the cotton. The glass cylinder is then positioned over the larvae for 24 seconds, removed for 3 seconds, and replaced for an additional 24 seconds. This

renders larvae unconscious and allows for their proper positioning prior to the application of tissue glue.

After scoring, a single larva is placed on the microscope slide and positioned dorsal side down. Histoacryl tissue glue is applied to the slide in a thin line next to the larva. The larva can then be gently picked up with No.5 forceps and placed in the glue. The glue is set by the application of 1xPBS using a micropipette. This step must be completed quickly, as larvae have a tendency to roll when they touch liquids, even when unconscious. Drops of 1xPBS are applied at the head of the larva on one side, at the tail on the same side, and then at the head and the tail of the other side. If 1xPBS is not dispensed precisely next to the larva and in small quantities the larva has a tendency to roll. If the larva rolls while the glue is setting, there is no way to reposition it so that it is dorsal side down. The procedure will need to be restarted.

Following application and setting of the tissue glue, the specimen is covered with several drops of 1xPBS and an incision is made through the cuticle in the centre of the larva. Internal organs and fat bodies can be removed to expose the heart. The cuticle cannot be pinned back in this setup, so it is trimmed away as well. Due to the resolution of the camera on the Bruker Bioscope Catalyst, one trachea is removed at this stage. This helps to orient the sample later. A photo of the dissection is also taken through the eyepiece of the dissecting microscope to aid in orienting the specimen at the AFM. Following dissection, specimens are bathed in 1xPBS at all times and are kept on ice until ready for analysis.

### 2.5.2 AFM setup

The AFM stage is mounted on a light microscope and the AFM scanning head is loaded. The probe can be visualized using the microscope and centred within the field of view. The microscope is connected to a camera and the field of view can be projected onto a computer monitor. The live view on the computer monitor can have a region of interest added to it, so once the probe is positioned a region of interest marker is placed on the screen where it is located. The scanning head is then removed and the microscope slide with the specimen is loaded onto the microscope. The heart can be located through the eyepieces using location cues from the photograph of the dissection as well as the missing trachea on one side. The tracheae are the easiest landmark to identify, so only having them on one side aids in positioning the larva. Once the heart is located, the field of view can be projected onto the computer screen and the heart can be aligned with the region of interest representing the location of the probe. The scanning head must be removed during the alignment of the heart because the light microscope associated with the AFM is inverted and the light source is generated from above. When the scanning head is in place, the light source is blocked, and it is difficult to locate features within the tissue.

Probes used for these experiments are colloidal probes from Novascan with the following specifications: 5 $\mu$ m borosilicate glass particle mounted on a silicon nitride cantilever, with spring constant 0.12 N/m.

Once the sample is aligned, the scanning head can be replaced on the AFM stage and the probe can be lowered onto the sample. This must be done with small step sizes (around 2 $\mu$ m) in order to prevent a false engage. A false engage can occur with colloidal

probes due to the weight of a large probe on a flexible cantilever. As the probe descends toward the sample, the resistance of the fluid around it forces the probe head up and the AFM interprets this as encountering the sample. Using small step sizes prevents large fluctuations in probe position.

When the probe engages the sample, force mapping can be performed. This technique measures the amount of force necessary to indent the tissue a set distance and generates a force curve for that point. Force curves are obtained in a grid of specified size, with a specified number of points sampled per side. Relevant settings for this system are a grid of 50-100 $\mu$ m with 16 points sampled per line. A physiologically relevant indentation depth is needed. For most trials, 2 $\mu$ m was selected.

## **2.6 Western blots**

Western blot protocol and solutions were based on the protocol outlined in Bourrouh et al (2016).

### **2.6.1 Western blot solutions**

The following solutions were used for Western blots: 2X sample buffer for grinding samples (2mL of 0.5M Tris-Cl, pH 6.8, 4mL of 10% SDS, 2mL of 100% glycerol, 0.31g of DTT (200mM), 20mg of bromophenol blue, double distilled water to 10mL) tris buffers to make gels (stacking gel buffer, 30g tris base in 500 mL of double distilled water, pH to 6.8; resolving gel buffer, 181.5g tris base, in 1 L of double distilled water, pH to 8.8), running buffer (TGS, 10x solution is 30g of tris base (25mM), 144g of glycine (192mM), 10g of SDS (1%) in 1 L of double distilled water), transfer buffer (TE, 1x solution, 15g of tris base (25mM), 72g of glycine (39mM), 750mL of MetOH (15%),

in 5L of double distilled water, stored at 4<sup>0</sup>C), TBST (10x solution, 100 mL of Tris-Cl (10mM), 87.66g of NaCl (150mM), 5mL of Tween20 (0.05%), in 1L of double distilled water).

### **2.6.2 General Western blot protocol**

Larval samples were placed in microcentrifuge tubes and flash frozen in liquid nitrogen. Samples were then ground in 2X sample buffer (30 $\mu$ L per larva). Ground samples were boiled at 65<sup>0</sup>C for 2.5 minutes, vortexed briefly, and spun down at max speed for 5 minutes. An 8% acrylamide gel was prepared. Gels were run at 120 V until the dye front had run off the gel. Gels were then transferred to nitrocellulose membrane using 350mA for one hour. Membrane was stained with Ponceau and imaged. Ponceau was rinsed off using water. The membrane was then blocked in 5% milk in 1xTBST for one hour. After blocking, membrane was left in primary antibody solution overnight at 4<sup>0</sup>C. After incubation in primary antibody solution, the membrane was washed for 15 minute intervals three times in 1xTBST. Membrane was then incubated with secondary antibodies at room temperature for between one and two hours. Blots were washed using 1xTBST for 20 minute intervals three times. Blots were then imaged using a Chemidoc imager and GE Healthcare ECL prime Western blotting detection reagents.

### **2.6.3 Westerns run**

Initial trials were performed on individual larvae. Individuals were ground in 30 $\mu$ L sample buffer, prepared as outlined in the general Western blot protocol, and 20 $\mu$ L was loaded into each well. Individual larvae did not yield consistent results as there is not enough protein in one sample (supplemental figures). For subsequent trials larvae were flash frozen in groups of 3 to 5. Westerns were performed on giant larvae, as well as genetic controls.

1 <sup>0</sup> antibody	Concentration	Supplier	2 <sup>0</sup> used
Pericardin	1/500	DSHB	goat $\alpha$ -mouse HRP conjugated
$\alpha$ -tubulin	1/2000	DSHB	goat $\alpha$ -mouse HRP conjugated

**Table 2.3: Antibodies used for Western blots**

Antibodies were diluted in 1xTBST prior to use. Primary antibodies were used at the stated concentrations. All secondary antibodies were used at 1 in 7000.

### 3. Results

#### 3.1 Generating and characterising giant larvae

##### 3.1.1 Generating giant larvae

Several unsuccessful attempts were made to generate giant larvae, with all crosses performed at 25<sup>0</sup>C. It was known that this phenotype was the result of a *snail* knockdown by UAS-*snail* RNAi in the prothoracic gland using *phmGal4* (Zeng, 2017). Transgene expression is controlled by the UAS/Gal4 system. UAS promoters are coupled with a transgene of interest and are activated by the Gal4 driver. Gal4 drivers are coupled with a tissue specific promoter, allowing for control over the spatial and temporal expression of transgenes. In this case, the RNAi against *snail* is expressed only in the prothoracic gland.

While the genetic manipulations required to generate giant larvae were known, the exact stocks that were used to generate this knockdown were unknown. Initial trials utilized the TRiP line generated for *snail* (Bloomington 28679, unpublished) and a commercially available *phmGal4* (Bloomington 26159). These crosses did not result in the developmental arrest necessary to generate giant larvae. Following the advice of the King-Jones lab at the University of Alberta who discovered this phenotype, *snail50003* and *snail50004* RNAi lines were obtained from VDRC, as well as *phm22Gal4* supplied by Michael B. O'Connor. Trials were performed using *daGal4*, a ubiquitous driver, and both VDRC *sna* RNAi lines. This cross was performed at 25<sup>0</sup>C and did not result in giant larvae. This confirmed that a ubiquitous driver was not sufficient, and a prothoracic gland specific driver was needed. *sna50003* and *sna50004* were then crossed to *phm22Gal4*. These crosses did not generate giant larvae, confirming that the recommendation of Zeng

(2017) to utilize *UAS-Dcr2* was necessary to achieve the desired phenotype. Dicer is involved in RNAi processing, and the inclusion of *UAS-Dicer2* in the background of an RNAi-induced gene knockdown results in enhanced RNAi efficiency. An initial attempt utilized *UAS-Dcr2,mCherry/CyO*, a second chromosome insert of *UAS-Dicer2*, and resulted in extremely delayed pupation, but not a larval arrest. This suggests that the second chromosome insert of *UAS-Dcr2* may not be as efficient as the X chromosome inserts, so the X chromosome insert *UAS-Dcr2;Pin/CyO* was recombined with the VDRC *snail* RNAi lines.

This led to the generation of giant larvae by performing recombination of *UAS-Dicer2* with *sna50003* RNAi (VDRC) and crossing the resulting recombinants to the prothoracic driver *phm22Gal4* (supplied by Michael B. O'Connor). When maintained at the correct temperature (25<sup>0</sup>C), the resulting giant larvae reach immense sizes after approximately 2 weeks of growth (figure 3.1). Giant larvae are able to live in this state for over a month. Some giant larvae arrest at the second instar stage of development, reportedly due to molting defects (Zeng, 2017). These larvae tend not to survive for more than a few days. A subset of giant larvae appear to demonstrate some sort of molting defect as well, with dark bands apparent on the cuticle near the posterior of the organism (figure 3.1).

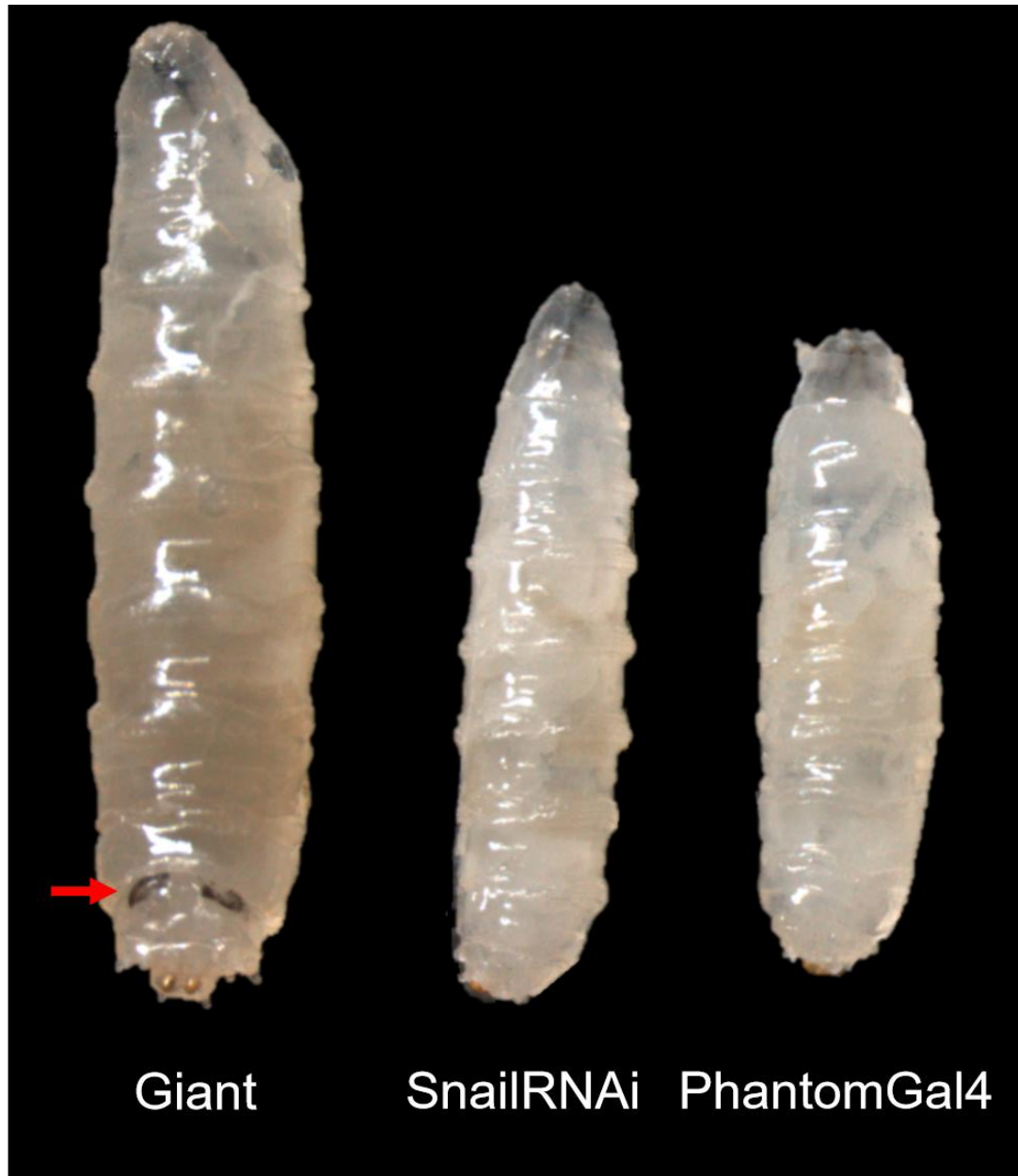


**Figure 3.1: Size comparison of giant larvae and genetic controls**

Giant is *sna50003, UAS-Dcr2 x phm22Gal4*. Controls are *sna50003, UAS-Dcr2/+* and *phm22Gal4/+*. Giant is 14 days old, controls are 4.5 day old wandering L3 larvae. Molting defect bands, indicated by red arrow, are visible on the giant larva.

### 3.1.2 Body size and mass measurements

Several measurements of size were obtained from images taken of giant larvae and genetic controls during dissection. Length and width measurements show a significant increase between giant larvae and both sets of genetic controls (figure 3.2).

The cross-sectional area of the heart lumen as a percentage of the cross-sectional area of the body cavity was calculated. This measure reveals greater than proportional growth of the heart in relation to total body size (figure 3.2).

The mass of giant larvae is significantly larger than control larvae (figure 3.2). On average, giant larvae are over twice as large as their control counterparts, with some individuals reaching masses of over three times that of the average control larva.

Dissection of giant larvae revealed a “fatty heart” phenotype not observed in control larvae (figure 3.3). A subset of giant larvae had fat deposits around the pericardial cells and heart tube. This deposit led to compression of the heart tube, revealed by deformed heart muscles (figure 3.3). Fatty hearts were observed in giant larvae more than 15 days old, suggesting this phenotype requires some time to develop.

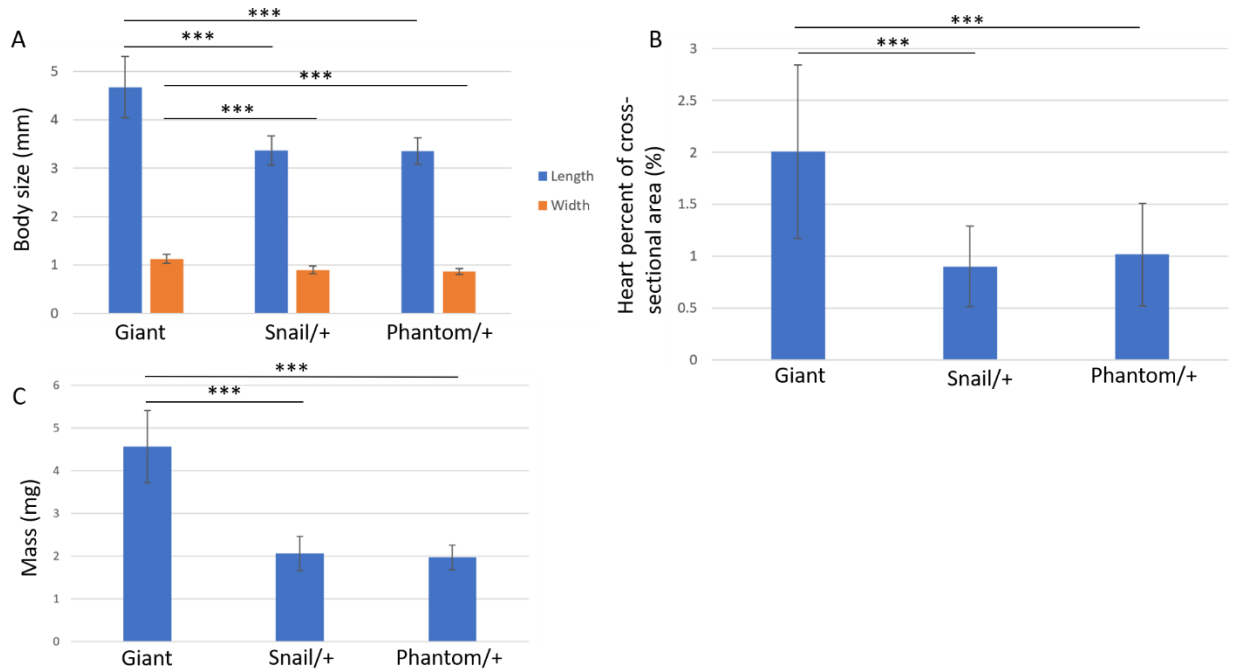


**Figure 3.2: Giant larval size and mass measurements**

A) Length and width measurements of giant larvae and wildtype (*yw*) controls. (n=24,18,17 for both A and B). B) gives a measure of the percentage of the cross-sectional area of the body that is occupied by the heart. C) Mass comparison of giant larvae and genetic controls. Error bars represent one standard deviation (n=25,13,13). \*\*\* represents  $P < 0.0002$ .

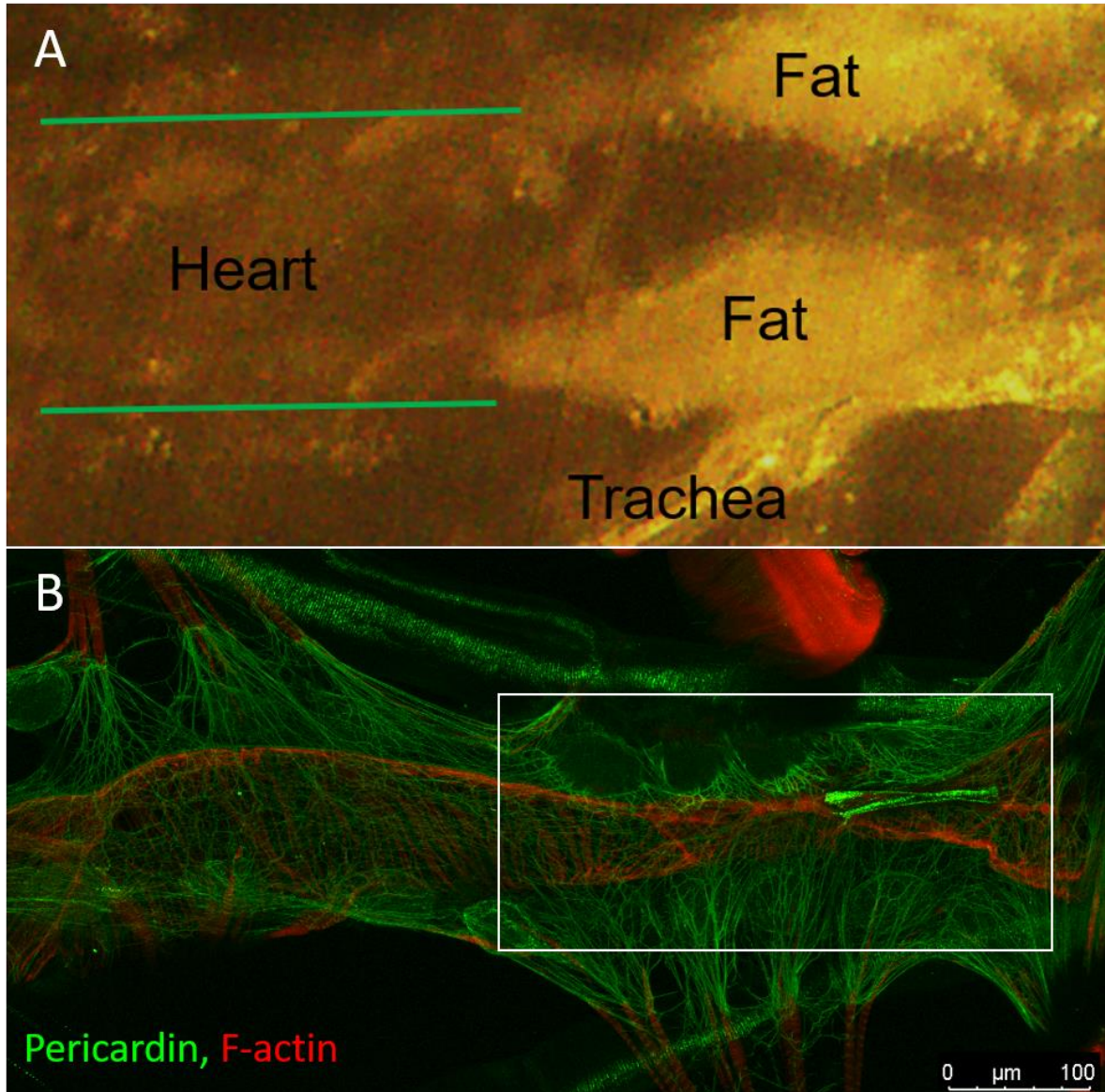


**Figure 3.3: Fatty heart phenotype in giant larvae**

A) Fat deposits are observed in a subset of giant larvae around the pericardial cells and heart tube. This leads to compression of the heart tube, shown within the white box in B). Refer to figure 3.4 for wildtype Pericardin and Actin morphology.

### 3.1.3 Core ECM component analysis

The ECM proteins Pericardin (heart specific collagen), Integrin and Collagen IV (Viking) were examined by immunolabelling and confocal microscopy (figure 3.4) to assess the impact of body size on the cardiac ECM. F-actin was also examined at the same time as these ECM proteins to assess the musculature of giant larvae.

Pericardin fibres appear more disperse and thicker in giant larvae when compared to controls. Quantification of Pericardin fibre thickness was performed in one individual of each genetic control, as well one giant larva. These measurements were obtained similarly to the method outlined in Vaughn et al (2018). This was a preliminary exercise, as the published methods do not appear reliable enough for unbiased assessment. Histograms showing the distribution of Pericardin fibre thickness are shown in figure 3.5. No clear trends are visible from this analysis.

Integrin labelling revealed that the overall structure of the heart is preserved in giant larvae - pericardial cells remain in close contact with the heart tube as is seen in control organisms (figure 3.4). However, these cells are more likely to be damaged during the dissection process in giant larvae due to the closer association of the fat bodies with the internal organs in these organisms.

Viking labelling shows that the Collagen IV network surrounding giant larval hearts is remarkably robust, showing no defects compared to controls (figure 3.4).

F-actin labelling revealed that alary muscles of giant larvae appear to be particularly robust. These muscles are often torn during dissection of wildtype larvae but were rarely damaged in giant larvae. Alary muscles are made up of several individual muscle fibres, and these fibres are spaced much further apart in giant larvae than in

controls. Additionally, it was observed that the muscles making up the heart tube maintained their organization despite the overgrowth of the organism (figure 3.4).

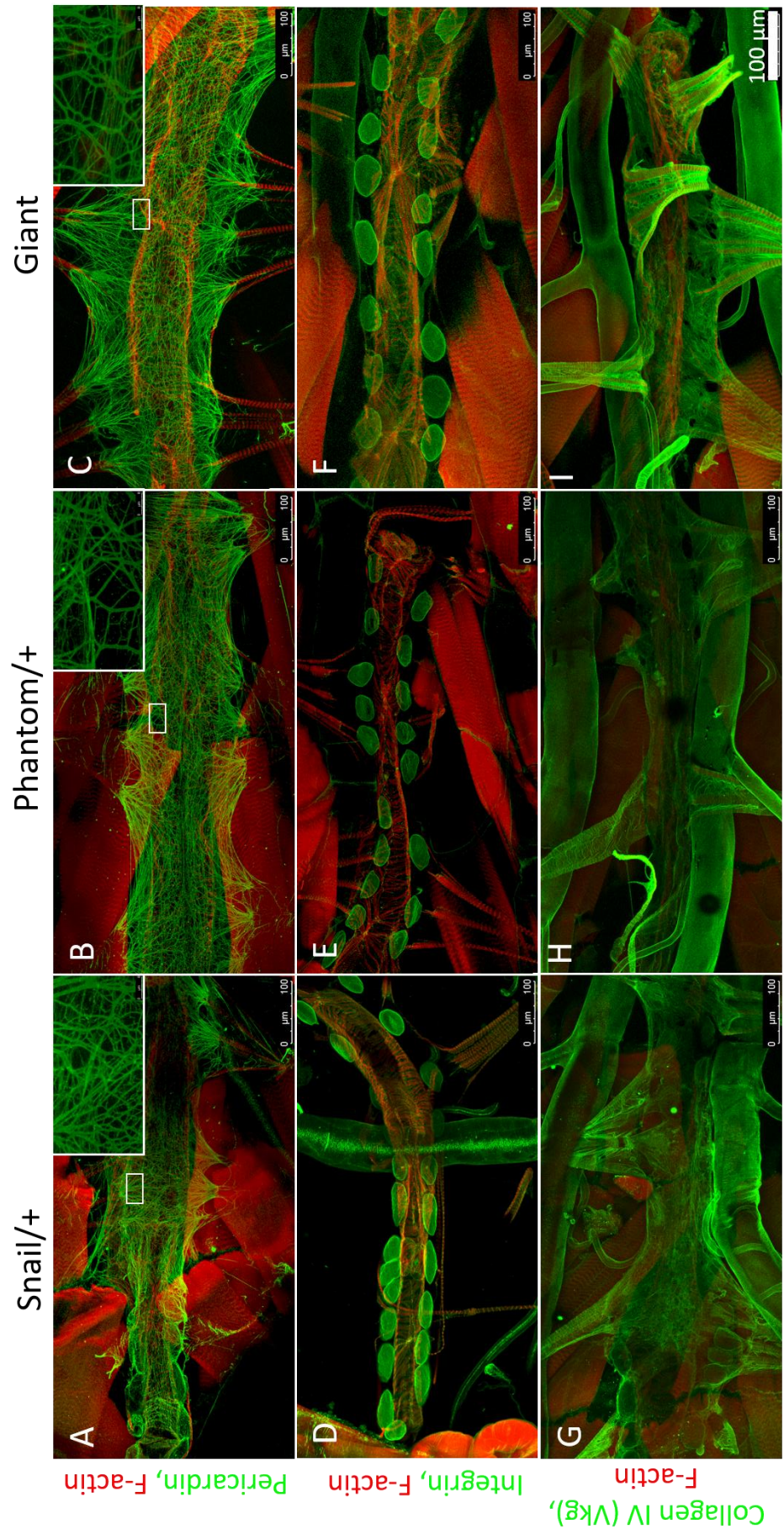


**Figure 3.4: Confocal analysis of ECM network**

The ECM proteins Pericardin (A-C), Integrin (D-F), and Viking (G-I) were immunolabelled in giants and genetic controls (*snailRNAi/+*, *phantom22Gal4/+*) and examined using confocal microscopy. Insets of Pericardin images were obtained using the 63x objective, with 4 times zoom. All other images were obtained using the 20x objective.

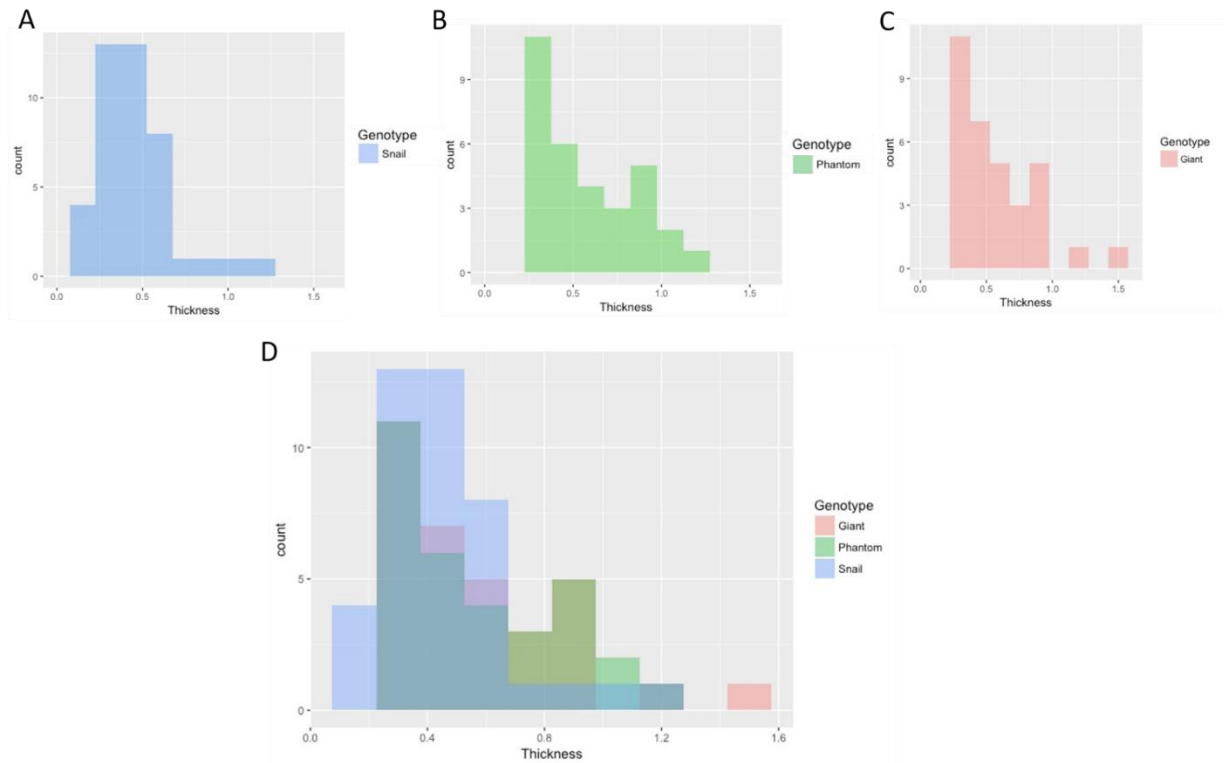


### Figure 3.5: Pericardin fibre thickness

Pericardin fibre thickness was quantified and plotted in a histogram for A) *snail*<sup>+</sup>, B) *phantom*<sup>+</sup>, and C) *giant* larvae. D) shows a merged histogram.

### 3.1.4 F-CHP in an invertebrate model

The 3-Helix denatured Collagen marker, 5-FAM conjugated Collagen hybridizing peptide (F-CHP) was obtained. This marker binds only to denatured Collagen strands and has been employed in vertebrate models to label regions undergoing ECM remodelling (Hwang et al, 2017). Its use had not been attempted in invertebrate models. Using the F-CHP marker, I tested the reactivity in an invertebrate model in order to assess the levels of remodelling occurring in control hearts when compared to a giant larval model.

Trials using F-CHP proved successful and demonstrate that it is appropriate for use in an invertebrate model. A small amount of denatured Collagen was observed in the larval *Drosophila* heart (figure 3.6), which could correspond to where remodelling is occurring. Refining the use of this marker will allow for quantification of levels of remodelling in giant larvae, in order to assess whether the increased load associated with a larger body size puts enough stress on the heart to cause elevated levels of Collagen remodelling.

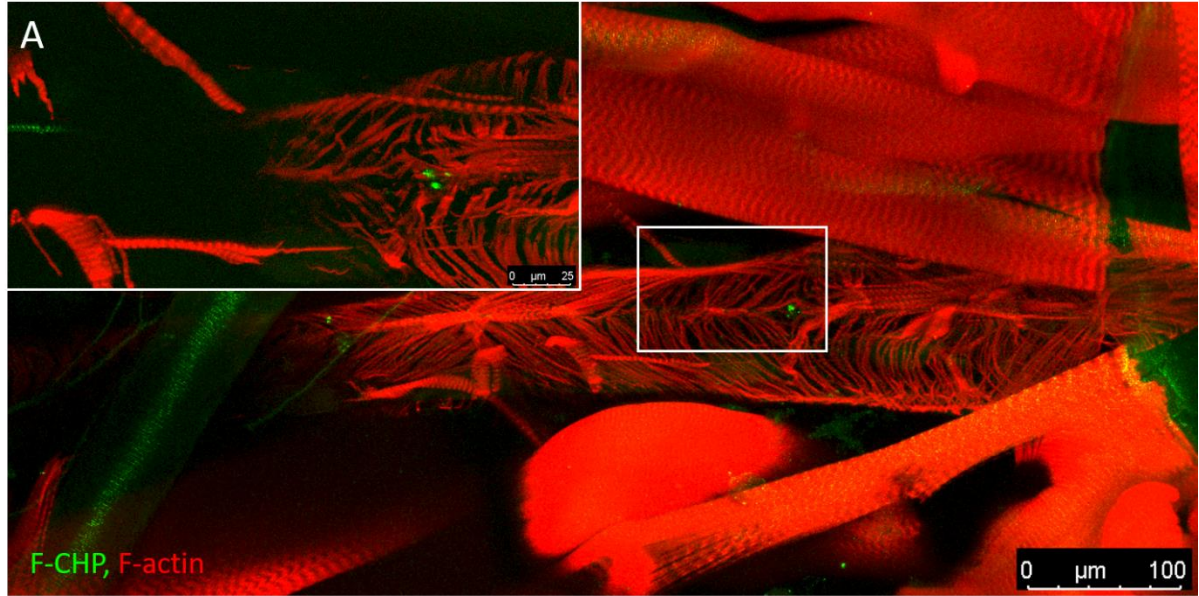


**Figure 3.6: 3-Helix denatured Collagen marker in an invertebrate model**

Wildtype (*yw*) larval *Drosophila* were dissected and immunolabelled with 20μM 3-Helix (F-CHP) marker. At this concentration a small amount of damaged Collagen that could correspond to an area of active remodelling is observed in larval hearts. Figure is at 20 times magnification, inset (top left) is 63 times magnification.

### 3.1.5 Functional analysis using OCT

Functional analysis of the heart was conducted on live larvae using optical coherence tomography (OCT) to assess the functional characteristics of giant larval hearts. Both videos of the heart beating as well as contraction cycle diagrams (examples shown in figure 3.8) were examined. Stills from OCT videos are shown in figure 3.7. Analysis of these videos reveals defects in the contraction cycle of giant larvae that are not present in controls. Control larvae are able to maintain a similar luminal shape through several contractions. Control larvae are also able to contract their hearts fully, with a very small luminal area during systole, as shown in figure 3.7. OCT videos also gave measures of luminal area and stroke volume (figure 3.9). These reveal that luminal area at both systole and diastole are significantly increased in giant larvae. There was also a significant increase in stroke volume, with giants exhibiting a 1.6-fold increase in stroke volume compared to controls (figure 3.9).

Live imaging revealed that giant larvae have an inability to contract the heart fully, resulting in a less than proportional increase in stroke volume for their body size (figure 3.9). While giant larvae are on average over twice as heavy as their control counterparts, the increase in stroke volume observed was only 1.6 times greater. Perhaps in compensation for this decrease in stroke volume, giant larvae have a significantly elevated heart rate ( $P=0.0008$ ) compared to controls (figure 3.10). While heart rate was elevated, rhythmicity of the heart is unchanged in giant larvae compared to control larvae (figure 3.10).

Giant larvae also show more variability in the shape of the heart lumen throughout several contraction cycles (data not shown). While a control larva is able to

maintain a relatively round lumen, both at diastole and systole, giant larvae often display an irregularly shaped lumen. Additionally, the shape of the lumen of giant larvae can be highly variable across different contraction cycles. This does not occur in wildtype organisms.

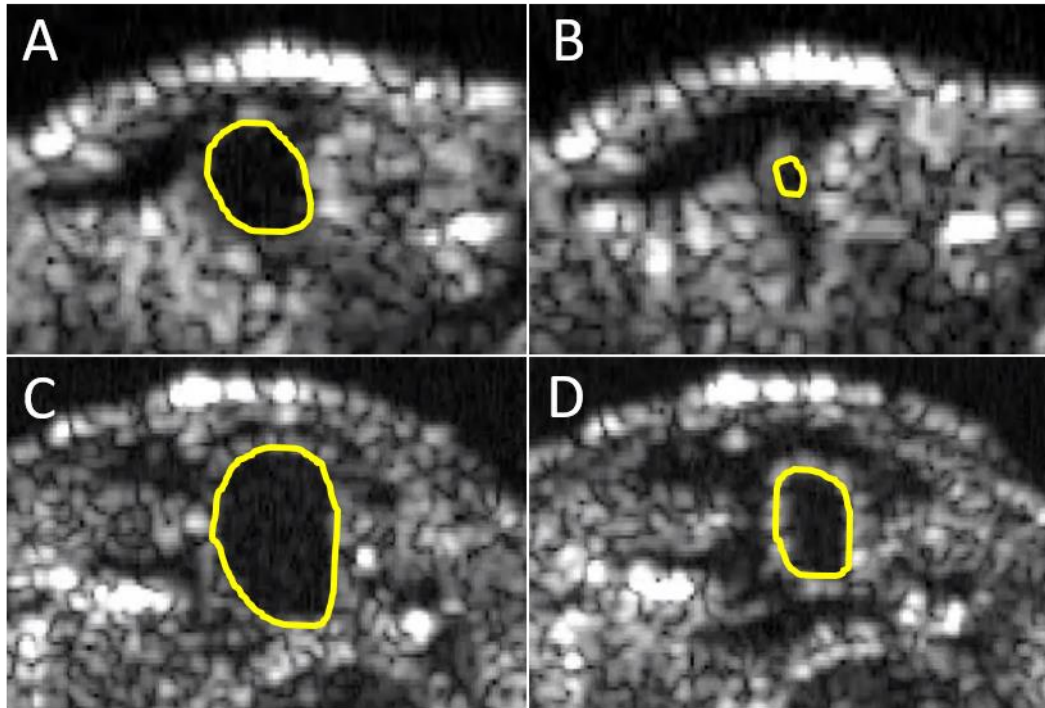


**Figure 3.7: Stills from OCT videos**

A) and B) show a wildtype (yw) heart lumen at diastole and systole respectively. C) and D) show a giant larval heart at both diastole and systole respectively. Giant larvae demonstrate an inability to contract fully during systole.

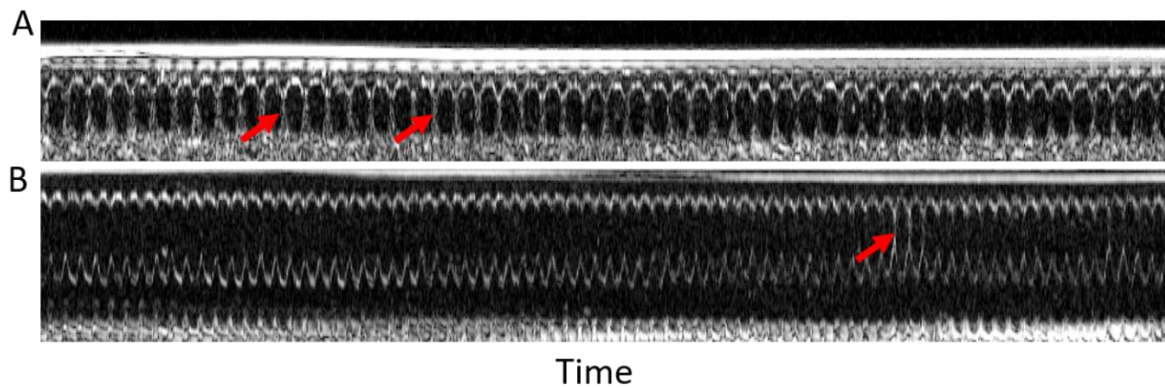


**Figure 3.8: Contraction cycles in one plane**

The top and the bottom edges at the midline of the heart were tracked through the duration of the 20 second OCT video clip and compiled into an image to assess the efficiency of the heart at contracting, as well as to provide a measure of heart rate and rhythmicity. Red arrows indicate full contraction of the heart walls. A) is wildtype control showing full contractions of the heart walls, while B) is giant larva showing an inability of the heart to contract effectively.

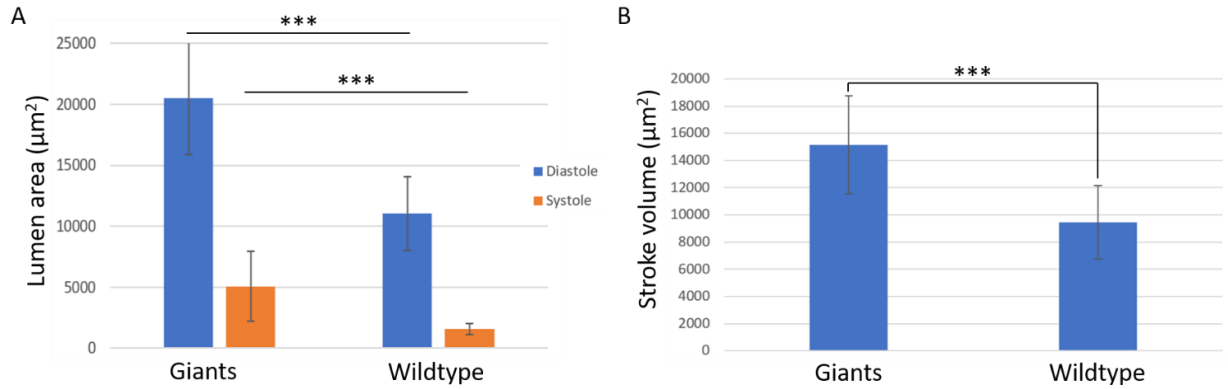


**Figure 3.9: Lumen area and stroke volume measurements obtained using OCT**

A) The area contained within the lumen of giant and wildtype (*yw*) hearts at diastole and systole. B) Stroke volume of giant and wildtype hearts, calculated as the change in luminal area between systole and diastole. Error bars represent one standard deviation (n=20,10 larvae. 3 heart cycles analysed from each). \*\*\* represents P<0.0001.

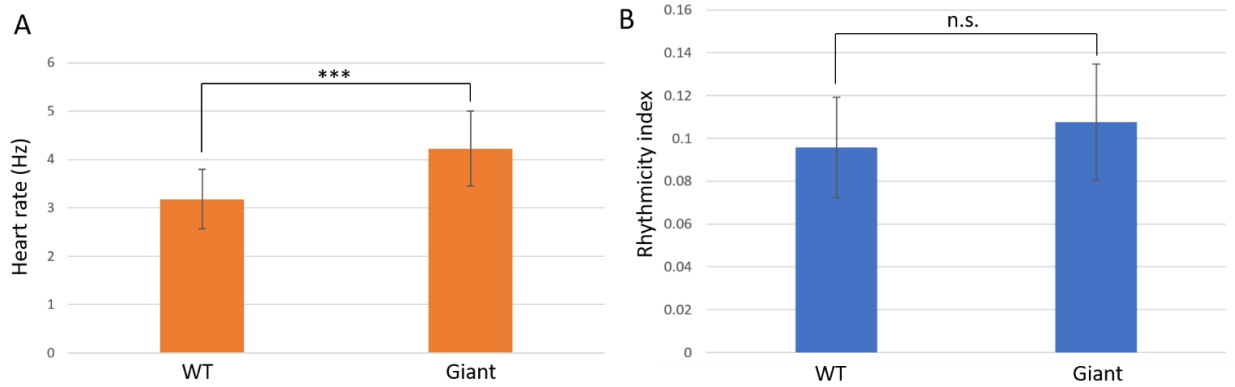


**Figure 3.10: Heart rate and rhythmicity of giant and wildtype hearts**

Heart rate and rhythmicity were calculated from OCT videos and contraction cycle diagrams respectively. A) shows that heart rate is significantly increased in giant larvae compared to wildtype controls ( $P=0.0008$ ). B) shows that rhythmicity index is not changed in giant larvae ( $P=0.233$ ). Error bars represent one standard deviation ( $n=10, 20$  larvae).

### 3.1.6 Western blot of Pericardin

Western blots were performed on giant larvae and genetic controls to determine whether giant larvae exhibit an increase in levels of the ECM protein Pericardin. These blots were probed with the ECM protein Pericardin, as well as the loading control  $\alpha$ -tubulin. Western blots show that it is possible to detect Pericardin with some reliability, and that two isoforms are present (figure 3.11). These isoforms correspond to different glycosylations of the protein. The predicted molecular weight of Pericardin is approximately 260kDa, but the higher band appears at around 200kDa and the lower band appears around 160kDa. This is consistent with the literature. Preliminary Western blot analysis reveals that Pericardin levels are highly variable across samples (figure 3.11). Results are too variable at this time to draw any conclusions.

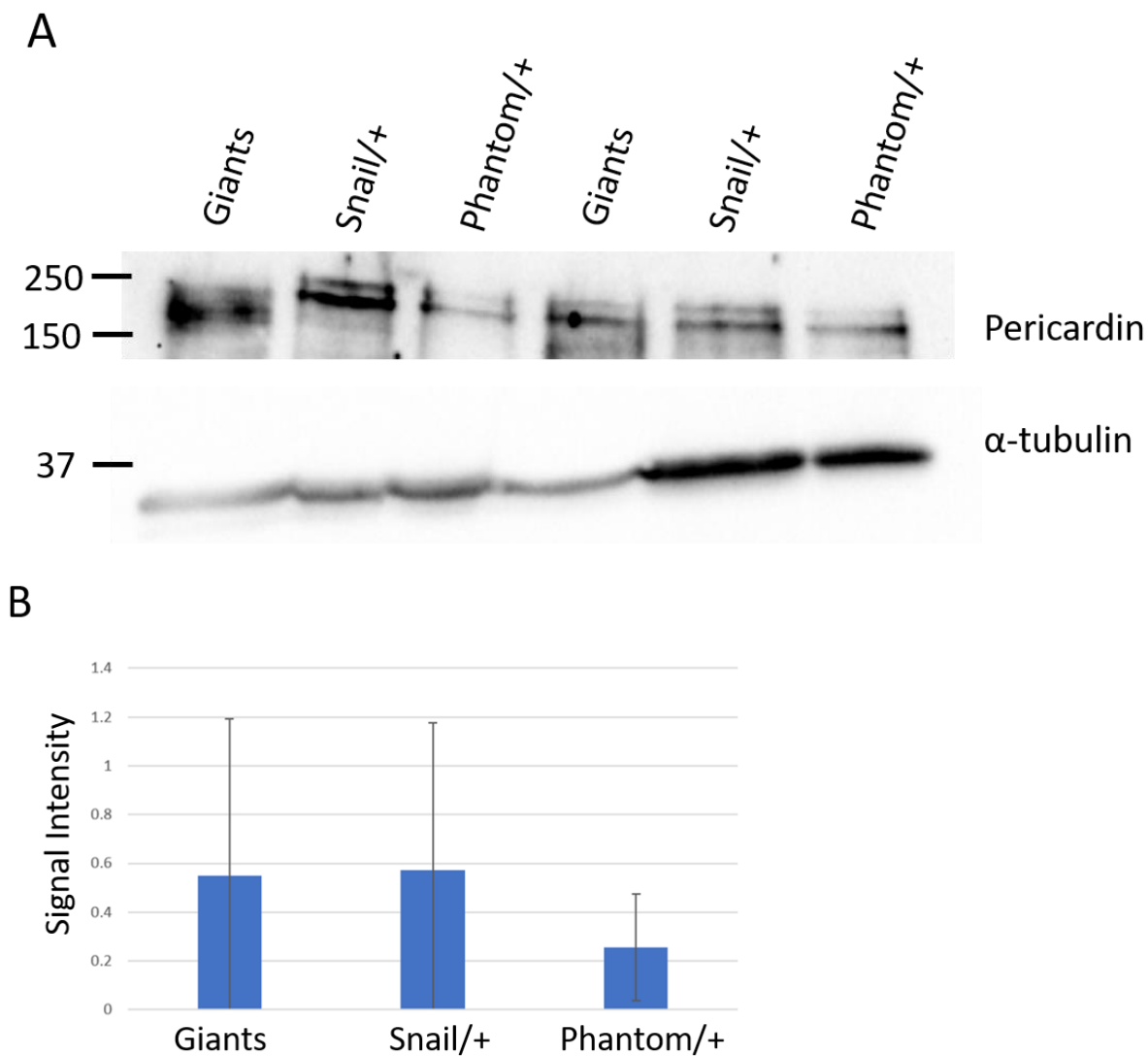


**Figure 3.11: Western showing Pericardin levels**

A) Western blot showing Pericardin levels in two sets of giant larvae and genetic controls. Each lane was loaded with 25 $\mu$ L of sample. Top blot probed with  $\alpha$ -Pericardin (~260kDa), bottom blot probed with  $\alpha$ - $\alpha$ -tubulin (~51 kDa). B) shows a high level of variability in standardised signal of intensity of Pericardin levels across samples.

## 3.2 Atomic force microscopy protocol development

### 3.2.1 Selecting an appropriate AFM

There are a variety of atomic force microscopes available on the McMaster campus. Several groups were met with, and trials were performed on two different microscopes to determine which was the best fit for *in situ* analysis of *Drosophila* heart tissue. The particular requirements of our system meant that several factors must be considered when selecting an appropriate AFM. First, living tissue must be kept hydrated with a buffer solution. This eliminated AFM setups that did not have the capability to make measurements in fluid. Second, it is necessary to be able to visualize where the probe will land on the specimen in order to obtain measurements from the heart tube and not from another tissue. This eliminated microscopes that did not have the capability of mounting the AFM stage on a light microscope, or a camera mounted within the scanning head or stage of the AFM. The combination of these factors eliminated several AFM setups, and left two possibilities: the Bruker Bioscope Catalyst at the Biointerfaces Institute or the MFP-3D Atomic Force Microscope belonging to the lab of Dr. Emily Cranston in the department of Engineering. Trials were performed using both of these AFM setups.

The Cranston lab AFM has two cameras. One is located above the cantilever to visualize the cantilever and probe as they descend towards the sample. The other camera is located below the stage and is directed up through the microscope slide. While it was possible to visualize the trachea of the dissected larva using this system and relatively easy to lower the probe onto the tissue, the resolution of the cameras did not allow for confidence in the placement of the probe. There is contrast between the trachea of the

*Drosophila* larva and its other tissue that does not exist with the heart. The only identifiable tissue using this setup was the trachea, so I could not be certain that my probe was landing on the heart using this system. Due to these concerns, this system was abandoned.

The Biointerfaces Institute AFM is used mainly for materials science applications. Due to the sensitive nature of this work, the stage of the microscope typically remains on the benchtop, not mounted on a light microscope. Several trials were performed in this orientation, in order to minimize the disruption to other users of the system. Aligning the probe with the heart without the aid of a light microscope proved challenging. Alignment with the AFM stage on the benchtop was attempted in several ways, including: dissecting on top of a grid sticker and marking the approximate location of the heart on the grid, photographing the dissection and drawing on the bottom of the slide near the area of interest, and using a handheld magnifying glass in an attempt to visualize the heart. All of these approaches were unsuccessful, so the AFM stage was mounted on an inverted light microscope for further tests. This allowed for visualization of the heart tube with great confidence, so this microscope was selected for our experiments. A labelled diagram illustrating the setup of this AFM is shown in figure 3.12.

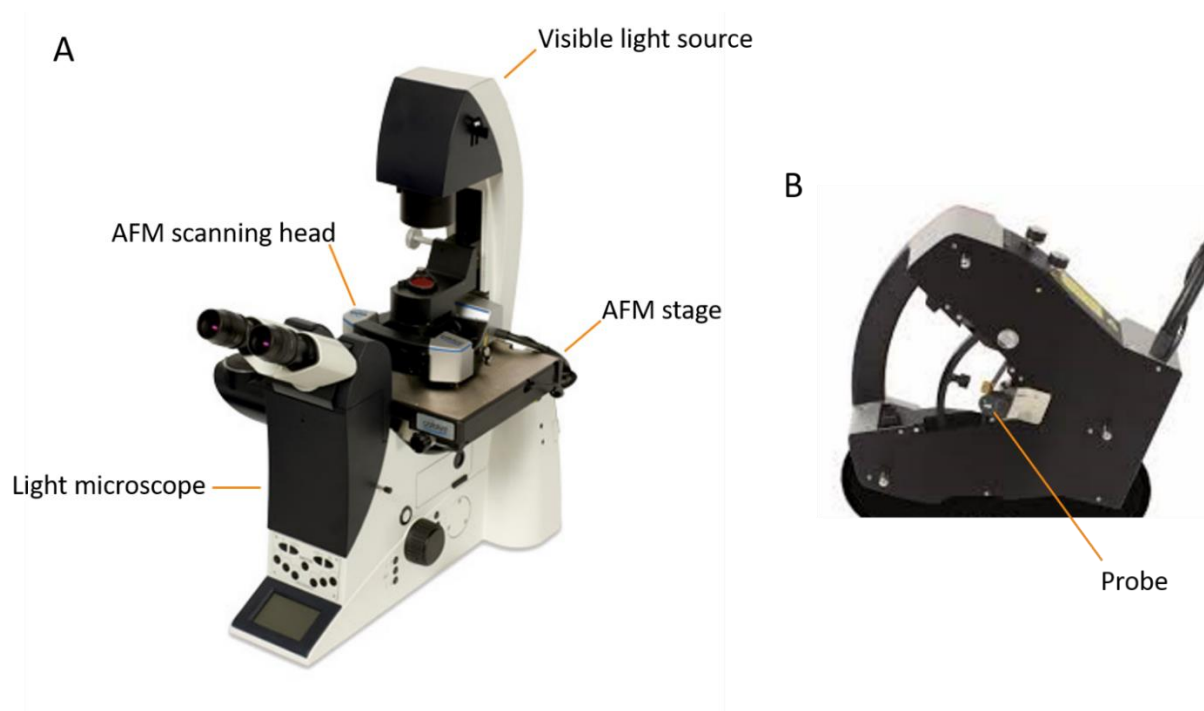


### Figure 3.12: Bioscope Catalyst

Key features of Bruker Bioscope Catalyst with AFM stage mounted on a light microscope labelled in A). A closeup view (from below) of the AFM scanning head shown in B) with location of probe labelled. (Adapted from Select Science and Bruker webinars.)

### 3.2.2 Dissection Protocol

When dissecting larvae to expose the heart, a dissection plate of 75mm x 50mm with raised sides to contain a well of buffering solution and pins to restrain the larva are typically used. Due to physical constraints of the Bruker Bioscope Catalyst at the Biointerfaces Institute, a standard microscope slide, 76mm x 26mm, is the only item that will fit under the AFM scanning head. A smaller dissection plate matching these dimensions was created, but the dissection pins were too high to allow for the lowering of the probe onto the sample. Several solutions were attempted for this problem. Microscope slides were coated in Sylgard and low-profile pins that could be embedded in the Sylgard matrix were created. These pins were still too high to allow lowering of the probe. Dissections using pins were then abandoned and the use of tissue glue was explored. Nexcare skin crack care glue was used first as it is commercially available and easy to obtain. This glue was found to be too weak to hold up to the strain of a dissection, leaving the samples detached from the microscope slide. Medical grade tissue glue was then explored. Histoacryl glue was ordered – this type of glue is typically used as liquid stitches and sets on contact with liquid. With this glue it is possible to immobilize a larva and carry out a dissection without it becoming separated from the microscope slide. These dissection parameters are successful, and are the standards used for all AFM trials. One small adjustment was needed to accommodate the range of the light microscope associated with the Biointerfaces AFM: prior to dissection, part of the microscope slide is scored using a diamond pen and removed. This is due to the limitations of the stage in scrolling from side to side over the sample. Unless the heart was perfectly centered on the slide it would not be possible to orient the probe above it. By removing a part of the slide

this allows for the heart to be aligned below the probe regardless of its position on the slide.

### **3.3.3 Placing AFM probe on heart**

Several issues were encountered when attempting to lower the probe onto the sample. Colloidal probes must be used for biological applications - colloidal probes possess a round probe, whereas traditional ‘sharp’ probes possess a triangular probe. When applied to tissues, colloidal probes ensure the sample will not be torn during analysis. The cantilevers used for biological applications of AFM tend to be quite flexible, and the colloidal probe mounted on the end of the cantilever is considerably heavier than a traditional sharp probe would be. The combination of these factors results in the end of the cantilever being dragged down by the probe when at rest, as well as the end of the cantilever being forced up by the resistance of the fluid surrounding the sample when being lowered. To circumvent this issue a very small step size (2 $\mu$ m) is needed when approaching the sample. If a larger step size is used, the cantilever is forced up and this triggers a false engage. After adjusting the step size of the engage settings, it was possible to successfully approach and engage with larval tissues, including heart tissue.

### **3.3.4 Collecting meaningful data**

When using colloidal probes, it is necessary to use the “Force volume” settings to generate a force map of the tissue. Using these settings, the probe is lowered onto the surface, where it indents a set depth into the tissue and generates a force curve for that point. This is repeated in a grid with dimensions set by the user. The recommended grid

size for these samples is 16x16 force curves, taken within a square between 50 and 100 $\mu$ m wide. The final size of the grid will depend on the nature of the data obtained while scanning. During trials, it is possible to calibrate the probe on a glass slide and position the probe above the heart with reasonable success. There are occasional issues visualizing the heart due to the glue used during the dissection. The light microscope associated with the AFM is an inverted microscope, meaning that the heart must be located through a layer of tissue glue, as well as a layer of body wall and cuticle. If there is a fold or a wrinkle in the glue, this can obstruct the view of the heart and make it difficult to ensure that the probe is positioned appropriately. The heart is a very narrow portion of the body cavity, so it is essential that the probe be positioned precisely. A dissection scope has been obtained to bring to Biointerfaces when collecting data so that a new dissection can simply be prepared on site. This will also allow for multiple specimens to be processed in one session.

Trials with this AFM have yielded only uncalibrated force maps, or calibrated force maps on dehydrated tissue. The Bruker technician has been aiding in some of these trials and is currently contacting a colleague with more experience analysing biological samples. There are several problems that must be addressed before meaningful data will be collected. This is a novel application of this technique and it is proving difficult to adapt atomic force microscopy to an *in situ* application on a micro scale.

## 4. Discussion

### 4.1 Characterising giant larvae

Giant larvae present a model for the study of obesity in *Drosophila*, with a focus on the impact of this phenotype on the function of the heart. To demonstrate that giant larvae are an effective model for such studies, their morphology must first be characterised.

Giant larvae have been successfully generated and are being characterised. Work to date has included immunolabelling of core ECM proteins, as well as live imaging to assess heart function. OCT imaging has revealed that giant larvae have defects in their ability to contract the heart effectively, leading to a less than proportional increase in stroke volume for their body mass. This is coupled with an increase in heart rate, which may be an attempt to maintain adequate cardiac output. In mammals, it is known that the mass of the heart scales proportionally to the mass of the organism (Dawson, 2014). Although allometric growth and scaling of the heart and cardiovascular system is well-characterized in mammalian systems, it has not been as thoroughly quantified in arthropod or other invertebrate models. There is some evidence that the mass of the circulatory system in a variety of insect species demonstrates an isometric relationship with body mass, and that the heart mass of the spiny lobster *Panulirus argus* is proportional to the average stroke volume of the organism (Polilov and Makarova, 2017; Maynard, 1960). While these findings support the conclusion that there is a greater than proportional increase in the luminal area of giant larvae, and a less than proportional increase in stroke volume, it is important to note that most studies performed using arthropod models are conducted during the adult life stage, rather than the larval stages.

This makes it difficult to conclude whether the growth observed in giant larvae is truly hyperallometric.

The lumens of giant larvae are often misshapen and unable to maintain a consistent shape through multiple contractions of the heart. This may be due to an increase in physical stress on the heart. Rhythmicity of the heart is unaffected which was unexpected given that arrhythmia is a characteristic of cardiovascular disease in an aging model (Vaughn et al, 2018). However, the *Drosophila* heart is known to undergo periods of rest. OCT analysis was restricted to periods of constant beating, which may create bias in the evaluation of rhythmicity.

Immunolabelling of ECM proteins has revealed that the matrix of giant larvae is robust and seems able to grow and remodel effectively despite the increase in body size. Visual inspection suggests that the Pericardin fibres of the giant larval ECM network are thicker and more disperse when compared to controls. This suggests there is a limited amount of distortion to the matrix to compensate for the increase in body size, but overall the Collagen matrix appears uncompromised. Pericardin fibre thickness is known to increase in cases of age-related fibrosis (Vaughan et al, 2018). However, the methods used to generate these measurements are ill-suited to unbiased quantification in giant larvae. The outlined method in Vaughan et al (2018) described making a limited number of measurements from single confocal z-stacks. Applied to larval samples, this would result in biased sampling. A modified protocol was applied to projected z-stacks to generate the histograms in figure 3.5 but should be improved upon before used for further quantification. In order to generate a more complete data set, it will be necessary to develop a more thorough method of quantification.

Integrin labelling has revealed that the pericardial cells remain closely associated with the heart tube, demonstrating that the gross architecture of the heart is mostly unaffected by the increase in body size of giant larvae. F-actin labelling reveals that the diameter of the heart tube tends to be significantly larger in giant larvae, and that alary muscles are large and robust. These muscles anchor the heart tube to the epidermis. Alary muscle fibres are also more spread out in giant larvae, suggesting that they are stretching to accommodate the increase in body size. It is common for alary muscles to tear during the dissection of wildtype and control larvae, but tearing rarely occurs during dissection of giant larvae, despite the added strain of the removal of fat bodies in this system. The fat bodies of giant larvae are large and more closely associated with many internal organs than those of wildtype larvae. Their removal requires more force than removing the fat bodies of control organisms. However, the musculature of giant larvae remains intact despite the added force required to perform a dissection. This demonstrates that the muscles or the connections supporting these muscles in giants are perhaps stronger than those of their control counterparts.

Interestingly, a characteristic of a weak extracellular matrix in the *Drosophila* heart is the inability to maintain appropriate connections between the heart tube and the alary muscles (Hollfelder et al, 2014). This is observed in cases where the ECM has been perturbed in some way and becomes unable to support the contractile nature of the heart tube, such as a Laminin B1 or Collagen mutant. These mutants display dissociation of the heart tube from both the alary muscles and the pericardial cells (Hollfelder et al, 2014). The opposite is observed in giant larvae. This larval overgrowth model demonstrates exceptionally robust connections between the heart tube and the alary muscles, which

may suggest that the cardiac ECM in giant larvae has more tensile strength than a typical matrix, potentially due to increased protein deposition and crosslinking, or fibrosis.

A subset of giant larvae begin to accumulate fat around the pericardial cells and heart tube. This “fatty heart” phenotype is not observed in wildtype larvae. Fat accumulation results in compression of the heart tube, which can be visualized by F-actin labelling. Fatty hearts are only observed in giant larvae that have been allowed to grow for long periods of time (>15 days), suggesting that the effects of body size on the larva are progressive, much like the affects of obesity and cardiovascular disease in mammals.

To further characterise the cardiac ECM of giant larvae, other core components of the ECM can be examined, including Laminin, Perlecan (Trol), and secreted protein acidic and rich in cysteine (SPARC). These proteins are all critical for the generation of an appropriate cardiac ECM, and their absence or misregulation results in cardiac dysfunction (Hollfelder et al, 2014; Hartley et al, 2016).

Laminin is known to be required to begin matrix assembly. Without its presence, a discontinuous ECM is generated. In the *Drosophila* heart, this results in a failure to assemble Collagen IV, the main structural component of the ECM, as well as Nidogen and Trol, both of which are required to help stabilize the matrix (Hollfelder et al, 2014). The distribution of Pericardin is also affected. This results in failure of alary muscles to make appropriately robust connections with the heart tube, leading to their dissociation from the heart tube (Hollfelder et al, 2014). This causes severe cardiac dysfunction and highlights the importance of Laminin in the formation of the ECM. Laminin is therefore of interest in the larval overgrowth model as its precise regulation is required for the formation of an appropriate ECM.

The protein SPARC has also been implicated in the formation of tissue fibrosis. SPARC normally plays a role in the stabilization of the basal lamina by its interaction with Collagen IV. In *Drosophila*, elevated levels of SPARC lead to a SPARC-dependent cardiomyopathy (Hartley et al, 2016). This cardiac dysfunction is characterised by impaired heart function, specifically a lengthened diastolic interval. SPARC is also known to contribute to the development of fibrosis in human cardiovascular disease, making it a candidate for the same process in *Drosophila* (Hartley et al, 2016). The presence of elevated SPARC levels in giant larvae would suggest that these larvae are experiencing elevated levels of fibrotic remodelling.

Trol is considered a core component of the ECM and plays a role in stabilizing the Collagen network of the cardiac ECM (Hollfelder et al, 2014). In Collagen IV mutants, Trol is unable to incorporate into the cardiac ECM, leading to a weak matrix. This matrix is unable to maintain the connections between the heart tube and the alary muscles, as well as the heart tube and the pericardial cells (Hollfelder et al, 2014). This again demonstrates the importance of an appropriately assembled ECM to heart function, as well as the importance of Trol in stabilizing the Collagen network, making it a candidate for study in giant larvae.

To generate a complete picture of the nature of the cardiac ECM in giant larvae, it will be beneficial to examine Laminin, SPARC and Trol levels and distribution in this system. Additionally, a marker specific for denatured collagen (5-FAM conjugated Collagen Hybridizing Peptide, F-CHP) has been obtained and tested. The F-CHP marker only binds to Collagen that is not part of the triple helix structure of a mature Collagen fibre, thus labelling only areas where remodelling is actively occurring. This allows for

visualization of the amount of remodelling occurring in this system. Trials performed with this marker have demonstrated that it is effective in invertebrates, and further experiments will quantify the amount of remodelling present in giant larvae compared to controls. Due to the increase in size of the body and the stress that this places on the heart, it is expected that giant larvae will display higher levels of remodelling than their wildtype counterparts.

#### **4.2 Biophysical analysis of *Drosophila* tissue**

An AFM protocol for the Bruker Bioscope Catalyst at the Biointerfaces Institute has been developed. While all parts of the protocol have been tested and work independently, a trial where the entire protocol works from start to finish has yet to occur. Some measurements have been obtained with an uncalibrated probe, or with a calibrated probe on a dehydrated sample. This highlights the difficulties of adapting this technique for *in situ* analysis on a micro scale, as most conventional biological uses of AFM are on a nano scale. Those that utilize AFM on tissue samples utilize samples removed from the body of the organism (Chen et al, 2018, Kim et al, 2014). Optimization of this technique for novel applications is incredibly time consuming, as is the analysis once a suitable protocol has been developed. An additional hurdle discovered is that most research groups that carry out AFM on biological samples do not do so themselves, they instead have a collaborator who carries out the analysis for them. The necessity of this system to carry out *in situ* analysis has compounded these issues. The unique nature of this system coupled with a lack of knowledgeable collaborators has created additional challenges in the creation of a protocol that meets the requirements of our system. Atomic force

microscopy is an incredibly specialized task and has a long lead time to optimize for novel applications. This is a limiting factor in its use for novel applications.

#### **4.2.1 Alternative methods of biophysical analysis**

As an alternative to AFM, the lab of Dr. Kari Dalnoki-Veress in the Physics and Astronomy department at McMaster measures elasticity of various substances by probing them with glass capillaries. This technique may offer a better way to determine the biophysical characteristics of the cardiac ECM as it is more adaptable and can be optimized for each application. The time to optimize this technique for a given application may be up to 12 months, again limiting its practical use.

### **4.3 Applications of a larval obesity model**

#### **4.3.1 Further characterisation of giant larvae**

In the long term, characterisation of more factors than the core components of the cardiac ECM must be carried out. Some important assays to conduct would be a triacylglyceride (TAG) assay to look at relative fat proportion in these larvae. This will inform how much of the increase in body mass observed in giant larvae is due to excess accumulation of fat.

The cause of death of giant larvae is currently unknown but could be due to prolonged hypoxia. It would be informative to discover the cause of death in these organisms in order to use them as a model for human disease progression. For example, assessment of hypoxia markers would address this variable. In *Drosophila*, oxygenation is carried out by the trachea, not the heart (Hayashi and Kondo, 2018). The beating of the

heart is required for movement of the hemolymph around the *Drosophila* body, which is required for the delivery of various metabolites, peptides, and nutrients (Rotstein and Paululat, 2016). Hypoxia is a well-known side effect of cardiovascular disease, and its presence in giant larvae would indicate that similar pathways are being activated in this model as are activated in mammalian disease states. HIF-1 $\alpha$  is the most commonly used marker for hypoxia in mammalian models, and an antibody for its *Drosophila* binding partner, Tango, is publicly available. Western blots conducted on giant larvae to assess Tango levels will give a measure of hypoxia levels in this system and could reveal whether this larval overgrowth model recapitulates mammalian cardiovascular disease.

Western blots can also be performed on giant larvae to assess relative levels of additional ECM proteins in order to determine if any are upregulated as a potential indicator of fibrosis. While Western blots conducted on Pericardin have revealed a striking level of variability between individuals even of the same genotype, several methods can be employed to improve Western blot results. For the sake of consistency readymade acrylamide gels can be purchased.

Pericardin is expressed only in the heart and may display variable Western results due to a relatively low abundance of protein in the sample. This may not be the case with other ECM proteins. Various other proteins are known to be upregulated during the progression of fibrosis in mammals, including the MMPs and TIMPs (El Hajj, El Hajj, 2018). In *Drosophila*, it has been shown that the MMPs have a major role in growth, as well as a minor role in development (Hughes, 2018). This supports the idea that upregulation of the *Drosophila* MMPs occurs in a larval overgrowth system. The ability

to quantify levels of these proteins would reveal the extent of ECM misregulation that is occurring in this model.

#### **4.3.2 Applications of biophysical techniques in *Drosophila* heart**

Biophysical analysis of giant larvae will be conducted to assess whether fibrosis is occurring in this model. Trials will continue on the Biointerfaces Institute Bioscope Catalyst in order to determine if it is possible to collect meaningful data on an *in situ* tissue preparation at the micro scale using atomic force microscopy. Most applications of atomic force microscopy occur at a nano scale, so the requirements of this model may be pushing the system past its capabilities. Trials will be conducted to determine if this is the case. Alternative options for measuring biophysical characteristics, such as the use of glass capillaries, will also be explored. This will determine whether AFM or another technique is more useful in the study of *in situ* biological specimens.

Once a method for measuring these properties has been chosen and optimized for this system, the elasticity of the tissue will be measured, and these measurements will provide a direct readout of the activity of the ECM in these organisms. A decrease in the elasticity of a system will be indicative of increased protein levels, as well as increased levels of crosslinking. Measuring tissue elasticity will help to quantify levels of maladaptive remodelling occurring in the system, and will allow for the direct quantification of levels of fibrosis.

### **4.3.3 Potential applications of larval overgrowth model**

Once the core components of the cardiac ECM have been satisfactorily characterised, and the levels of remodelling and fibrosis in giant larvae quantified, matrix perturbations will be carried out. There are a variety of proteins that are known to be involved in remodelling that are also upregulated during the progression of fibrosis, including Lysyl Oxidase (LOX), the MMPs, and the TIMPs (El Hajj, El Hajj, 2018). LOX is crucial for the crosslinking of Collagen and is known to be upregulated when the heart is stressed. The degree of crosslinking in the matrix influences its stiffness and increased levels of crosslinking can prevent Collagen degradation (El Hajj, El Hajj, 2018). By knocking down the expression of LOX, the amount of crosslinking in the matrix will be reduced and could help to alleviate some of the functional problems generated by decreased matrix flexibility.

MMPs and TIMPs are involved in the regulation of remodelling and are known to be upregulated during cardiac stress and in disease states (El Hajj, El Hajj, 2018). Upregulation of these proteins leads to a loss of regulation of the cardiac ECM, leading to functional consequences. Ablation or reduction of their function may restore the balance of protein turnover in the ECM.

### **4.4 Concluding thoughts**

The giant larval model presents a unique opportunity to study the effects of body size on the cardiac ECM, and the impacts this has on heart function. The cardiac ECM is of critical importance to the function of the heart as a whole and is known to undergo maladaptive remodelling in response to cardiac stress, called fibrosis. Fibrosis of the

heart is a characteristic of cardiovascular disease progression in humans, so the study of its development and progression is of utmost importance. The giant larval overgrowth model demonstrates cardiac dysfunction as a result of increased body size. Visual assessment suggests that the Pericardin matrix is slightly distorted by the increased growth, but the matrix reveals remarkable plasticity in its ability to adapt to increased body size. Matrix composition is not the only important factor involved in fibrotic remodelling. Levels of protein crosslinking are also known to increase in these contexts (El Hajj, El Hajj et al, 2018). Perturbation of genes involved in the mediation of remodelling, both in terms of protein deposition and turnover as well as crosslinking, will reveal the pathways the heart employs to achieve such plasticity in the matrix.

The biophysical characteristics of a tissue, including elasticity, are critical when discussing the impact of fibrotic remodelling on a tissue. However, measurements of these characteristics are mostly indirect and are conducted by quantifying protein levels or levels of crosslinking, rather than measuring the properties of the tissue itself. This led to the development of an atomic force microscopy protocol in order to assess these characteristics directly. Applying this to *in situ* tissues will allow an unprecedented level of quantification of the level of fibrosis in a system. This proved to be a complicated undertaking and more work is necessary in this area to determine whether this method is the most useful for biophysical analysis in this system.

The benefit of working on an overgrowth model in *Drosophila* is the ease of performing genetic manipulations and treatments. When this model is fully characterised, it will be possible to perform manipulations of ECM components of interest in order to attempt to treat specific issues that occur in this system.

## 5. References

- Heart Disease in Canada, *Government of Canada*. (2017).  
<https://www.canada.ca/en/public-health/services/publications/diseases-conditions/heart-disease-canada.html>
- Obesity in Canadian Adults, 2016 and 2017, *Statistics Canada*. (2018).  
<https://www150.statcan.gc.ca/n1/pub/11-627-m/11-627-m2018033-eng.htm>
- Alanis, J., Gonzalez, H., and Lopez, E. The Electrical Activity of the Bundle of His. (1958). *J. Physiol.*, 142, 127-140.
- Birse, R., Choi, J., Reardon, K., Ocorr, K., Bodmer, R., Oldham, S. High fat diet induced obesity and heart dysfunction is regulated by the TOR pathway in *Drosophila*. (2010). *Cell Metab.*, 12(5): 533–544. doi:10.1016/j.cmet.2010.09.014.
- Bogatan, S., Cevik, D., Demidov, V., Vanderploeg, J., Panchbhaya, A., Vitkin, A., and Jacobs, R. Talin is required continuously for cardiomyocyte remodeling during heart growth in *Drosophila*. (2015). *PLoS One*, 10(6): e0131238.
- Bourouh, M., Dhaliwal, R., Rana, K., Sinha, S., Guo, Z., and Swan, A. Distinct and overlapping requirements for cyclins A, B, and B3 in *Drosophila* female meiosis. (2016). *G3*, 6(11), 3711-3724. doi: 10.1534/g3.116.033050.
- Brent, J.R., Werner, K.M., and McCabe, B.D. *Drosophila* larval NMJ dissection. (2009). *J. Vis Exp.*, 4(24). doi:10.3791/1107
- Brogiolo, W., Stocker, H., Ikeya, T., Rintelen, F., Fernandez, R., and Hafen, E. An evolutionarily conserved function of the *Drosophila* insulin receptor and insulin-like peptides in growth control. (2001). *Current Biology*, 11(4), 213-221.
- Cevik, D., Acker, M., Arefi, P., Ghaemi, R., Zhang, J., Selvaganapathy, P.R., Dworkin, I., and Jacobs, R. Chloroform and desflurane immobilization with recovery of viable *Drosophila* larvae for confocal imaging. (2019). *J Insect Physiol*, 13, 117:103900. doi: 10.1016/j.jinsphys.2019.103900.
- Chen, X., Wanggou, S., Bodalia, A., Wang, L., Li, X., and Huang, X. A feedforward mechanism mediated by mechanosensitive ion channel Piezo1 and tissue mechanics promotes glioma aggression. (2018). *Neuron*, 100(4):799-815.e7. doi:10.1016/j.neuron.2018.09.046.
- Cieslik, K. A., Taffet, G. E., Carlson, S., Hermosillo, J., Trial, J., & Entman, M. L. Immune-inflammatory Dysregulation Modulates the Incidence of Progressive Fibrosis and Diastolic Stiffness in the Aging Heart. (2011). *Journal of Molecular and Cellular Cardiology*, 50(1), 248–256. doi:10.1016/j.yjmcc.2010.10.019.
- Dawson, T.H. Allometric Relations and Scaling Laws for the Cardiovascular System of Mammals. (2014). *Systems*, 2, 168-185. doi:10.3390/systems2020168

- Diop, S.B., Birse, R.T., and Bodmer, R. High fat diet feeding and high throughput triacylglyceride assay in *Drosophila melanogaster*. (2017). *J Vis Exp.*, 127. doi: 10.3791/56029.
- El Hajj, E.C., El Hajj, M.C., Ninh, V.K., and Gardner, J.D. Inhibitor of Lysyl Oxidase Improves Cardiac Dysfunction and the Collagen/MMP Profile in Response to Volume Overload. (2018). *Am J Physiol Heart Circ Physiol.* 315(3):H463-H473. doi:10.1152/ajpheart.00086.2018. Epub 2018 May 18.
- Fan, D., Creemers, E.E., and Kassiri, Z. Matrix as an Interstitial Transport System. (2014). *Circulation Research*, 114, 889-902. doi:10.1161/CIRCRESAHA.114.302335.
- Gomez, I.M., Rodriguez, M.A., Santalla, M., Kassis, G., Coleman Lerner, J.E., Aranda, O., Sedan, D., Ferrero, P. et al. Inhalation of marijuana affects *Drosophila* heart function. (2019). *Biol Open*, pii: bio.044081. doi:10.1242/bio.044081.
- Hartley, P., Motamedchaboki, K., Bodmer, R., and Occor, K. SPARC-Dependent Cardiomyopathy in *Drosophila*. (2016). *Circ Cardiovasc Genet*, 9, 119-129. doi:10.1161/CIRCGENETICS.115.001254.
- Hollfelder, D. and Reim, F.M. Distinct functions of the Laminin  $\beta$  LN Domain and Collagen IV during cardiac extracellular matrix formation and stabilization of alary muscle attachments revealed by EMS mutagenesis in *Drosophila*. (2014). *BMC Developmental Biology*, 14(26).
- Hughes, C. J. R., and Jacobs, J. R. Dissecting the Role of the Extracellular Matrix in Heart Disease: Lessons from the *Drosophila* Genetic Model. (2017). *Veterinary Sciences*, 4(2), 24. doi:10.3390/vetsci4020024.
- Gaetano, J. Holm-Bonferroni sequential correction: an excel calculator (1.2). (2013). doi: 10.13140/RG.2.1.3920.0481
- Hayashi, S., and Kondo, T. Development and function of the *Drosophila* tracheal system. (2018). *Genetics*, 209(2), 367-380. doi: 10.1534/genetics.117.300167
- Hwang, J., Huang, Y., Burwell, T.J., Peterson, N.C., Connor, J., Weiss, S.J., Yu, S.M., Li, Y. *In Situ* imaging of tissue remodelling with Collagen hybridizing peptides. (2017). *ACS Nano*, 11, 9825-9835. doi:10.1021/acsnano.7b03150
- Jourdan-LeSaux, C., Zhang, J., and Lindsey, M. L. (2010). Extracellular Matrix Roles During Cardiac Repair. *Life Sciences*, 87(13-14), 391–400. doi:10.1016/j.lfs.2010.07.010.
- Kim, S., Jeibmann, A., Halama, K., Witte, H.T., Walte, M., Matzat, T., Schillers, H., Klambt, C. et al. ECM stiffness regulates glial migration in *Drosophila* and mammalian glioma models. (2014). *Development*, 141(16), 3233-3242. doi:10.1242/dev.106039.
- Kirmizis, D. and Logothetidis, S. Atomic force microscopy probing in the measurement of cell mechanics. (2010). *International Journal of Nanomedicine*, 5, 137-145.

- Lebleu, V.s., Macdonald B., and Kalluri, R. Structure and Function of Basement Membranes. (2007). *Exp Biol Med*, 232, 1121-1129. doi:103181/0703-MR-72.
- Maynard, D. Heart rate and body size in the spiny lobster. (1960). *Physiological Zoology*, 33(4), 241-251.
- Meschiari, C., Ero, O. K., Pan, H., Finkel, T., and Lindsey, M. L. (2017). The Impact of Aging on Cardiac Extracellular Matrix. *GeroScience*, 39(1), 7–18. doi:10.1007/s11357-017-9959-9.
- Mouw, J.K., Ou, G., and Weaver, V.M. Extracellular matrix assembly: a multiscale deconstruction. (2014). *Nature reviews*, 15, 771-785.
- Oldham, S., Stocker, H., Laffargue, M., Wittwer, F., Wymann, M., and Hafen, E. The *Drosophila* insulin/IGF receptor controls growth and size by modulating PtdInsP<sub>3</sub> levels. (2002). *Development*, 129, 4103-4109.
- Poirier, P., Giles, T.D., Bray, G.A., Hong, Y., Stern, J.S., Pi-Sunyer, F.X., and Eckel, R.H. Obesity and Cardiovascular Disease: Pathophysiology, Evaluation, and Effect of Weight Loss. (2006). *Circulation*, 113(6), 898-918. doi:10.1161/CIRCULATIONAHA.106.171016.
- Poliliv, A., and Makarova, A. The scaling and allometry of organ size associated with miniaturization in insects: A case for Coleoptera and Hymenoptera. (2017). *Scientific Reports*, 7:43095. doi:10.1038/srep43095.
- Raza, Q.S., Vanderploeg, J., and Jacobs, R. Matrix Metalloproteinases are required for membrane motility and lumenogenesis during *Drosophila* heart development. (2017). *PLoS One*, 12(2):e0171905. doi:10.1317/journal.pone.0171905.
- Rotstein, B. and Paululat, A. On the morphology of the *Drosophila* heart. (2016). *J. Cardiovasc Dev Dis.*, 3(2), 15. doi:10.3390/jcdd3020015.
- Rotstein, B., Post, Y., Reinhardt M., Lammers, K., Buhr, A., Heinisch, J.J., Meyer, H., and Paululat, A. Distinct domains in the matricellular protein Lonely heart are crucial for cardiac extracellular matrix formatin and heart function in *Drosophila*. (2018). *J. Biol. Chem.* 293(20), 7864-7879. doi:10.1074/jbc.M117.817940.
- Sessions, A. O., Kaushik, G., Parker, S., Raedschelders, K., Bodmer, R., Van Eyk, J.E., and Engler, A.J. Extracellular matrix downregulation in the *Drosophila* heart preserves contractile function and improves lifespan. (2017.) *Matrix Biology*, 62, 15-27. doi:10.1016/j.matbio.2016.10.008.
- Shih, H.T. Anatomy of the action potential in the heart. (1994). *Texas Heart Institute Journal*, 21, 30-41.
- Travers, J.G., Kamal, F.A., Robbins, J., Yutzey, K.E., and Blaxall, B.C. Cardiac Fibrosis – The Fibroblast Awakens. (2016). *Circulation Research*, 118, 1021-1040. doi:10.1161/CIRCRESAHA.115.306565

Vanderploeg, J. and Jacobs, J. R. Talin is required to position and expand the luminal domain of the *Drosophila* heart tube. (2015). *Developmental Biology*, 405, 189-201. doi:10.1016/j.ydbio.2015.04.024.

Vaughn, L., Marley, R., Miellet, S., and Hartley, P. The impact of *SPARC* on age-related cardiac dysfunction and fibrosis in *Drosophila*. (2018). *Experimental Gerontology*, 109, 59-66.

Walker, C.A., and Spinale, F. The structure and function of the cardiac myocyte: a review of fundamental concepts. (1999). *The Journal of Thoracic and Cardiovascular Surgery*, 118, 375-382.

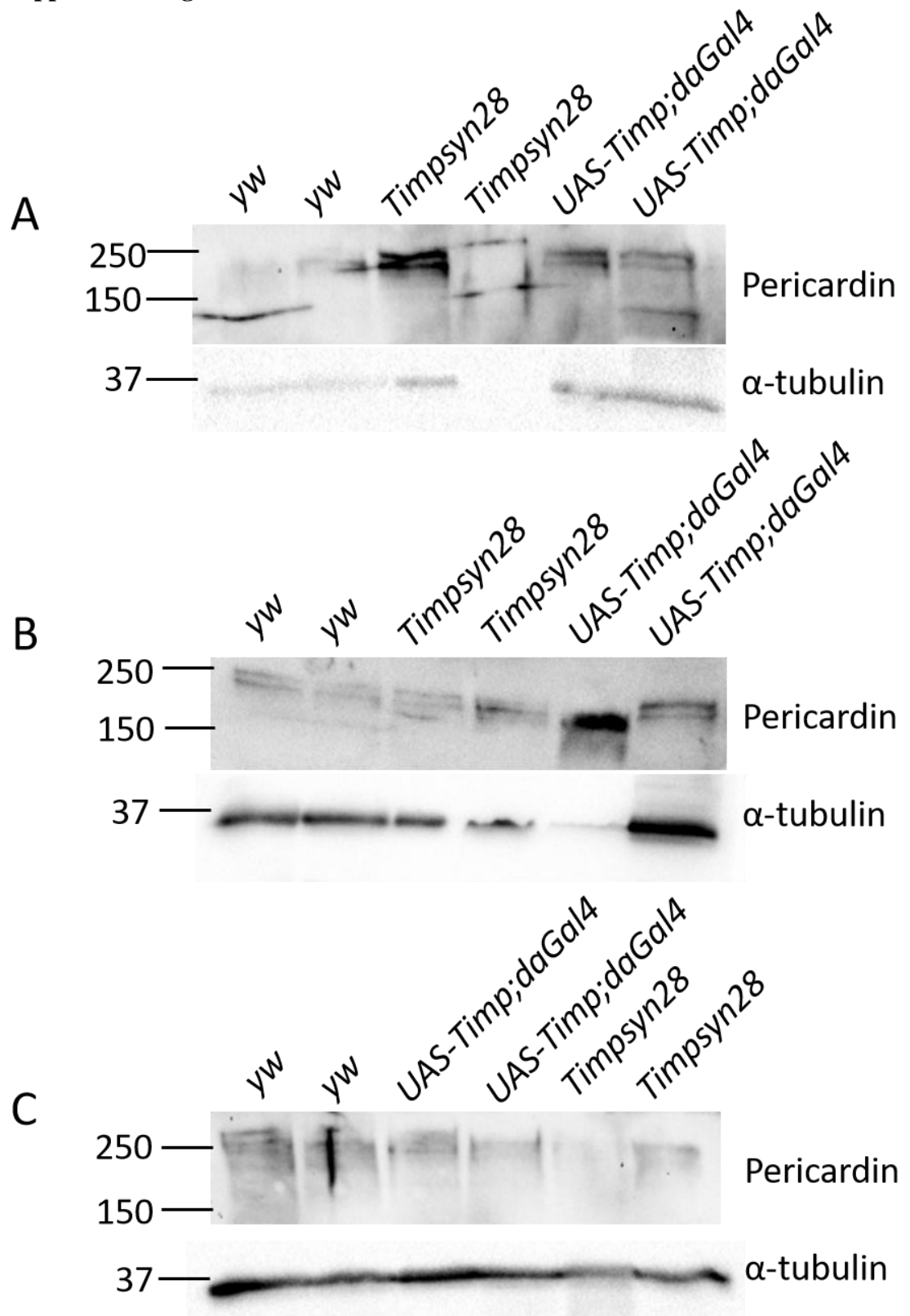
Weidemann, F., Hermann, S., Stork, S., Neimann, M., Frantz, S., Lange, V., Beer, M., Gattenlohner, S., Voelker, W., Ertl, G., and Strotmann, J.M. Impact of Myocardial Fibrosis in Patients with Symptomatic Severe Aortic Stenosis. (2009). *Circulation*, 120, 577-584. doi:10.1161/CIRCULATIONAHA.108.847772

Wilmes, A., Klinke, N., Rotstein, B., Meyer, H., and Paululat, A. Biosynthesis and assembly of the Collagen IV-like protein Pericardin in *Drosophila melanogaster*. (2018). *Biology Open*, 7, bio030361. doi:10.1242/bio.030361.

Xin, X., Li, Z., Leng, Y., Neu, C.P., and Calve, S. Knockdown of the pericellular matrix molecule Perlecan lowers in situ cell and matrix stiffness in developing cartilage. (2016). *Developmental Biology*, 418(5), 242-247.

Zeng, J. (2017). Characterizing new players in regulating the production of the steroid hormone ecdysone during larval development of *Drosophila melanogaster*. *Doctoral thesis, University of Alberta*.

## 6. Supplemental figures



**S1: Westerns of individual larvae**

Westerns were performed on individual larvae in order to determine if individual variations in Pericardin levels could be detected. Blots yielded wildly inconsistent results, making quantification of Pericardin levels across individuals impossible. A), B), and C) are representative blots showing the variability observed both between blots and between samples.